# ANOMALOUS CURRENT IN PERIODIC LORENTZ GASES WITH INFINITE HORIZON

N. CHERNOV AND D. DOLGOPYAT

Abstract. We study electrical current in two-dimensional periodic Lorentz gas in the presence of a weak homogeneous electric field. When the horizon is finite, i.e. the free flights between collisions are bounded, the resulting current $\mathbf{J}$ is proportional to the voltage difference $\mathbf{E}$, i.e. $\mathbf{J} = \frac{1}{2}\mathbf{D}^*\mathbf{E} + o(\|\mathbf{E}\|)$, where $\mathbf{D}^*$ is the diffusion matrix of the Lorentz particle moving freely without electrical field (see a mathematical proof in [11]). This formula agrees with classical Ohm's law and the Einstein relation. Here we investigate the more difficult model with infinite horizon. We find that infinite corridors between scatterers allow the particles (electrons) move faster resulting in an abnormal current (causing 'superconductivity'). Precisely, the current is now given by $\mathbf{J} = \frac{1}{2}\mathbf{D}\mathbf{E}\big|\log\|\mathbf{E}\|\big| + \mathcal{O}(\|\mathbf{E}\|)$, where $\mathbf{D}$ is the 'superdiffusion' matrix of the Lorentz particle moving freely without electrical field. This means that Ohm's law fails in this regime, but the Einstein relation (suitably interpreted) still holds. We also obtain new results for the infinite horizon Lorentz gas without external fields, complementing recent studies by Szasz and Varju [28].

## 1. Introduction

Lorentz gas is a popular model in mathematical physics introduced in 1905, cf. [20], for the purpose of describing the motion of electrons in metals. The original model consisted of small (point-like) non-interacting particles moving in space and bouncing off fixed rigid bodies (scatterers). In mathematical studies the scatterers are usually positioned at sites of a periodic lattice, and the particles make specular reflections off their surfaces.

We study a two-dimensional periodic Lorentz gas, which reduces to a dynamical system generated by a point-like particle moving on a plane

The authors acknowledge the hospitality of Erwin Schrödinger Institute in Vienna, where this work began, and N. Chernov acknowledges the hospitality of University of Maryland, where this work was finished. We thank P. Balint for reading the manuscript and making many valuable suggestions and T. Gilbert for helpful discussions. N. Chernov was partially supported by NSF grant DMS-0652896. D. Dolgopyat was partially supported by NSF grant DMS-0555743.

$\mathbb{R}^2$ and bouncing off a periodic array of fixed convex figures (playing the role of scatterers). In most of this paper, we assume that the 'horizon' is infinite, i.e. there are infinitely long corridors stretching between the scatterers; see Figure 1 in Section 2.

Mathematical studies of the 2D periodic Lorentz gases, without external fields, i.e. where the particle moves freely between collisions, began in 1970 by Sinai [27]. Due to the lack of external forces, this model is a Hamiltonian system preseving an equilibrium (Liouville) measure. The speed of the particle remains constant and is traditionally set to one. Due to the periodicity of the array of scatterers, the dynamics reduces to a billiard on a torus with a finite set of fixed scatterers.

Sinai [27] proved that if the scatterers are convex domains with $C^3$ smooth boundaries with nonvanishing curvature, then the resulting billiard flow and collision map are hyperbolic (i.e. have non-zero Lyapunov exponents), ergodic, and K-mixing. Later they were shown to have Bernoulli property [19]. Thus this model is highly chaotic in every mathematical sense.

However, global statistical properties of the periodic Lorentz gas happen to depend on whether the horizon is finite or infinite, i.e. whether the free path between collisions with scatterers is bounded or not. The finite horizon case is much better understood, we review its main properties below.

Let $\tilde{\mathcal{D}}$ denote the area available to the moving particle (the plane $\mathbb{R}^2$ minus the union of scatterers). Since the scatterers are located periodically, the whole plane can be covered by replicas of a certain region (fundamental domain) $\mathcal{K} \subset \mathbb{R}^2$ so that $\tilde{\mathcal{D}}$ is in turn the union of copies of bounded domain $\mathcal{D} = \tilde{\mathcal{D}} \cap \mathcal{K}$. Now the field-free Lorentz gas reduces to a planar billiard on the finite table $\mathcal{D}$ with periodic boundary conditions.

For the billiard in $\mathcal{D}$, we denote by $\mathbf{q}(t) \in \mathcal{D}$ and $\mathbf{v}(t) \in \mathbb{S}^1$ the position and velocity of the moving particle at time $t$. The billiard generates a flow $\Phi^t$ on compact phase space $\Omega = \mathcal{D} \times \mathbb{S}^1$, which preserves Liouville measure $\mu_0$ (the latter is just a uniform measure on $\Omega$). The collision space is defined by

$$\mathcal{M} = \big\{(\mathbf{q}, \mathbf{v})\colon \mathbf{q} \in \partial\mathcal{D},\ \|\mathbf{v}\| = 1,\ \mathbf{v} \text{ points inside } \mathcal{D}\big\}$$

and the collision map $\mathcal{F}\colon \mathcal{M} \to \mathcal{M}$ takes a collision point to the next collision point.

Let $(r, \varphi)$ denote the standard coordinates in $\mathcal{M}$, where $r$ is the arc length parameter on $\partial\mathcal{D}$ and $\varphi \in [-\pi/2, \pi/2]$ the angle between the outgoing velocity vector $\mathbf{v}$ and the outward normal vector to $\partial\mathcal{D}$ at the collision point $\mathbf{q}$, cf. [4, 13]. The map $\mathcal{F}$ preserves a smooth probability

measure $\nu_0$ on $\mathcal{M}$ given by

$$d\nu_0 = c_\nu \cos\varphi \, dr \, d\varphi, \qquad c_\nu = \big[2 \cdot \text{length}(\partial\mathcal{D})\big]^{-1} \tag{1.1}$$

here $c_\nu$ is the normalizing factor. For every $X \in \mathcal{M}$ let

$$\tau(X) = \min\{t > 0 \colon \Phi^t(X) \in \mathcal{M}\} \tag{1.2}$$

denote the time of the first collision of the trajectory starting at $X$.

For the particle moving in the infinite domain $\tilde{\mathcal{D}}$, we denote by $\tilde{\mathbf{q}}(t)$ its position at time $t$ and by $\tilde{\mathbf{q}}_n$ its position at its $n$th collision with $\partial\tilde{\mathcal{D}}$. Let $\boldsymbol{\Delta}_n = \tilde{\mathbf{q}}_{n+1} - \tilde{\mathbf{q}}_n$ denote the displacement vector between collisions. (Note that we use tildas for notation related to the dynamics in the unbounded region $\tilde{\mathcal{D}}$.)

In all theorems, except Theorem 3, we assume that the initial position $\tilde{\mathbf{q}}(0)$ and the initial velocity $\mathbf{v}(0)$ are chosen according to the Liouville measure $\mu_0$ in $\mathcal{D} \times \mathbb{S}^1$. All the results remain valid if the initial distribution is smooth and has compact support.

**Theorem 1** ([3, 4])**.** *Suppose that the particle moves freely without external fields.*
(a) $\tilde{\mathbf{q}}(t)/\sqrt{t}$ *converges, as* $t \to \infty$*, to a normal distribution, i.e*

$$\tilde{\mathbf{q}}(t)/\sqrt{t} \Rightarrow \mathcal{N}(\mathbf{0}, \mathbf{D}^*)$$

*with a non-degenerate covariance matrix* $\mathbf{D}^*$ *called* diffusion matrix*.*
(b) *The latter is given by* Green-Kubo formula*:*

$$\mathbf{D}^* = \frac{1}{\bar{\tau}_0} \sum_{n=-\infty}^{\infty} \nu_0\big(\boldsymbol{\Delta}_0 \otimes \boldsymbol{\Delta}_n\big) \tag{1.3}$$

*where* $\bar{\tau}_0 = \nu_0(\tau)$ *is the mean free path given by*

$$\bar{\tau}_0 = \nu_0(\tau) = \frac{\pi \, \text{Area}(\mathcal{D})}{\text{length}(\partial\mathcal{D})} \tag{1.4}$$

*and* $\mathbf{u} \otimes \mathbf{v}$ *denotes the 'tensor product' of two vectors, i.e. the product of the column-vector* $\mathbf{u}$ *and the row-vector* $\mathbf{v}$*.*

This theorem was derived in [3, 4]. Young [31] showed that the series (1.3) converges exponentially fast. See a recent exposition in [13, Chapter 7]; for the proof of (1.4) see [13, Section 2.13].

Next consider 2D periodic Lorentz gases with finite horizon where the particle is subject to a small homogeneous (i.e. constant in time and space) external field $\mathbf{E}$. To keep the particle's energy fixed, one couples the field $\mathbf{E}$ with Gaussian thermostat [11, 12, 24], so that the motion between collisions is governed by equations

$$d\tilde{\mathbf{q}}/dt = \mathbf{v}, \qquad d\mathbf{v}/dt = \mathbf{E} - \zeta\mathbf{v}, \tag{1.5}$$

where $\zeta = \langle \mathbf{E}, \mathbf{v} \rangle / \|\mathbf{v}\|^2$. The friction term $\zeta \mathbf{v}$ is called the Gaussian thermostat, it ensures $\|\mathbf{v}\| = \text{const}$ at all times; again we will assume that $\|\mathbf{v}\| = 1$.

Let us fix the direction of $\mathbf{E}$ and regard $\varepsilon = \|\mathbf{E}\|$ as a small parameter of the model. Again, due to periodicity of the scatterers, we get a new flow, call it $\Phi_\varepsilon^t$, on the same phase space $\Omega = \mathcal{D} \times \mathbb{S}^1$, and a new collision map, $\mathcal{F}_\varepsilon \colon \mathcal{M} \to \mathcal{M}$; the spaces $\Omega$ and $\mathcal{M}$ remain independent of $\mathbf{E}$. The collision time function (1.2) now depends on $\varepsilon$, i.e. $\tau = \tau_\varepsilon$. Also, for every $X \in \mathcal{M}$ we denote by

$$\mathbf{\Delta}_\varepsilon(X) = \tilde{\mathbf{q}}_1 - \tilde{\mathbf{q}}_0 \tag{1.6}$$

the displacement of the particle moving in the infinite domain $\tilde{\mathcal{D}}$ before its next collision at $\partial\tilde{\mathcal{D}}$.

**Theorem 2** ([11, 12])**.** *Let $\tilde{\mathbf{q}}(t)$ be the position of the particle in the finite horizon Lorentz gas with a small external field $\mathbf{E}$ coupled with a Gaussian thermostat* (1.5)*. Then*
(a) *For small enough $\varepsilon = \|\mathbf{E}\|$, the map $\mathcal{F}_\varepsilon$ is hyperbolic; it preserves a Sinai-Ruelle-Bowen (SRB) measure (a steady state) $\nu_\varepsilon$, which is ergodic and mixing. It is singular but positive on open sets. The flow $\Phi_\varepsilon^t$ also preserves an SRB measure $\mu_\varepsilon$ on $\Omega$, which is ergodic, mixing, and positive on open sets. The electrical current*

$$\mathbf{J} = \lim_{t\to\infty} \tilde{\mathbf{q}}(t)/t = \mu_\varepsilon(\mathbf{v}) = \nu_\varepsilon(\mathbf{\Delta}_\varepsilon)/\bar{\tau}_\varepsilon$$

*is well defined; here $\bar{\tau}_\varepsilon = \nu_\varepsilon(\tau_\varepsilon)$ is the mean free path (or the average intercollision time), for which we have $\bar{\tau}_\varepsilon = \bar{\tau}_0 + \mathcal{O}(\varepsilon)$ as $\varepsilon \to 0$.*
(b) *We have*

$$\mathbf{J} = \tfrac{1}{2}\, \mathbf{D}^* \mathbf{E} + o(\varepsilon), \tag{1.7}$$

*where $\mathbf{D}^*$ is the diffusion matrix of Theorem 1.*
(c) *We have the following weak convergence, as $t \to \infty$:*

$$\frac{\tilde{\mathbf{q}}(t) - \mathbf{J}t}{\sqrt{t}} \Rightarrow \mathcal{N}(0, \mathbf{D}_\varepsilon^*),$$

*where $\mathbf{D}_\varepsilon^*$ is the corresponding* diffusion matrix*.*
(d) *The diffusion matrix is continuous in $\varepsilon$ at $\varepsilon = 0$:*

$$\mathbf{D}_\varepsilon^* = \mathbf{D}^* + o(1). \tag{1.8}$$

This theorem was proved in [11, 12] and extended to more general external forces in [6, 7].

Note that (1.7) can be regarded [11, 12] as classical *Ohm's law*: the electrical current $\mathbf{J}$ is proportional to the voltage $\mathbf{E}$ (to the leading order). The fact that the electrical conductivity, i.e. $\frac{1}{2}\mathbf{D}^*$ in (1.7), is

proportional to the diffusion matrix $\mathbf{D}^*$ is known in physics as *Einstein relation* [11, 12]. Observe that due to (1.8) the Einstein relation can be also restated as

$$\mathbf{J} = \tfrac{1}{2}\,\mathbf{D}^*_\varepsilon \mathbf{E} + \text{higher order terms}. \tag{1.9}$$

According to Theorem 2, the position of the particle can be roughly approximated by

$$\tilde{\mathbf{q}}(t) \approx \big[\tfrac{1}{2}\,\mathbf{D}^* + o(1)\big]\mathbf{E}\,t + \big[(\mathbf{D}^*)^{1/2} + o(1)\big] Z\sqrt{t}, \tag{1.10}$$

where $Z$ denotes the 2D standard normal random vector. The first term in (1.10) represents the steady drift of the particle, and the second – its chaotic diffusion.

Next we turn to the Lorentz particle moving in an external field without thermostat, i.e. the equations of motion are now very simple:

$$d\tilde{\mathbf{q}}/dt = \mathbf{v}, \qquad d\mathbf{v}/dt = \mathbf{E}. \tag{1.11}$$

However, this case is far more difficult than the previous one, because the particle is allowed to accelerate ('heat up'), so that the system no longer preserves a finite measure. If we choose the coordinate frame so that the $x$ axis is directed along the field $\mathbf{E}$, i.e. $\mathbf{E} = (\varepsilon, 0)$, then we can expect that $x(t) \to \infty$ and $\|\mathbf{v}(t)\| \to \infty$, as $t \to \infty$. More precisely, as the total energy

$$H = \tfrac{1}{2}\,\|\mathbf{v}(t)\|^2 - \langle \mathbf{E}, \tilde{\mathbf{q}}(t)\rangle = \tfrac{1}{2}\,\|\mathbf{v}(t)\|^2 - \varepsilon x(t)$$

is conserved, we have $x(t) \sim \|\mathbf{v}(t)\|^2$. It was long conjectured in physics literature that $x(t) \sim t^{2/3}$ and $\|\mathbf{v}(t)\| \sim t^{1/3}$, see references in [10, 9], but mathematically this model was investigated only very recently [9].

Assume that the particle is confined to the half plane $\{x \ge 0\}$ and experiences mirror reflections off the line $x = 0$. This model is actually known in physics as Galton board [18].

**Theorem 3** ([9])**.** *Suppose that the initial condition of the particle has a smooth compactly supported density on an energy surface $\{H = H_0\}$ where $H_0$ is sufficiently large.*
(a) *There is a constant $c_\diamond > 0$ such that $c_\diamond t^{-2/3} x(t)$ converges, as $t \to \infty$, to a random variable with density*

$$\frac{3}{2\Gamma(2/3)} \exp\left[-z^{3/2}\right], \quad z \ge 0.$$

(b) *The constant $c_\diamond$ is given by*

$$c_\diamond = \left(\frac{32\,\|\mathbf{E}\|^5}{81\langle \mathbf{D}^*\mathbf{E}, \mathbf{E}\rangle}\right)^{1/3}.$$

**Remark.** (c) *There exists a limiting distribution for* $t^{-2/3}y(t)$*, too, but it is given by a more complicated formula* [10].

Thus, depending on the type of external forces, the particle moving in the finite horizon Lorentz gas can exhibit different scaling behavior. However in all cases the transport coefficients satisfy simple relations and are expressed in terms of the diffusion matrix $\mathbf{D}^*$. We note that the matrix $\mathbf{D}^*$, given by (1.3), is a highly non-explicit function of the geometry of the scatterers. In fact, there are indications [8] that $\mathbf{D}^*$ cannot be differentiable with respect to the geometric characteristics of the scatterers (e.g., their centers or diameters). But given $\mathbf{D}^*$, one can compute other transport coefficients quite easily.

This concludes our introductory review of the Lorentz gases with finite horizon. In the next section we turn to the more difficult case of infinite horizon.

## 2. Statements of results

This paper is a part of a larger project to extend all the above results to the infinite horizon periodic Lorentz gases. In this paper we present analogues of Theorems 1 and 2, leaving the extension of Theorem 3 for a later publication.

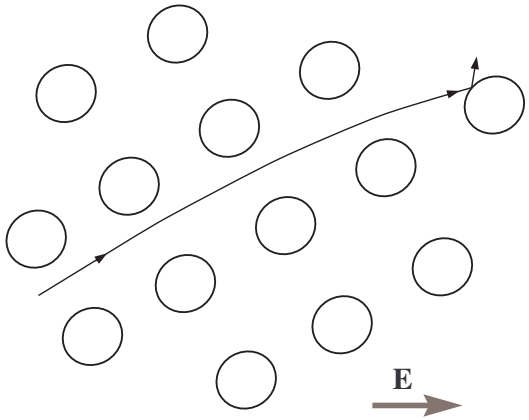


Figure 1. A particle moving along an infinite corridor between scatterers: due to the external field $\mathbf{E}$ its trajectory bends and hits a scatterer.

**Field-free Lorentz gas.** In the infinite horizon case the particle can move freely without collisions along infinite corridors stretching between the scatterers, see Figure 1. Now its long-term behavior is quite

different from the one described in Theorem 1. The first manifestation of this difference is that the Green-Kubo series (1.3) defining the diffusion matrix in the finite horizon case, now diverges because its central term is infinite:

$$\nu_0\big(\boldsymbol{\Delta}_0 \otimes \boldsymbol{\Delta}_0\big) = \infty.$$

(The main technical result of our paper, however, asserts that all the other terms, $\nu_0\big(\boldsymbol{\Delta}_0 \otimes \boldsymbol{\Delta}_n\big)$ for $n \neq 0$, are finite and decay exponentially in $n$; see Proposition 9.1.)

Because the diffusion matrix defined by (1.3) turns infinite, the particle exhibits an abnormal diffusion (often called 'superdiffusion'). Namely the correct scaling factor in the Central Limit Theorem is now $\sqrt{t \log t}$, rather than $\sqrt{t}$. This fact was conjectured long time ago, and a partial proof was published by Bleher [2] in 1992. A complete mathematical proof, for the discrete time, appeared in 2007 due to Szasz and Varju [28]. Their main result is

**Theorem 4** ([28])**.** *Let $\tilde{\mathbf{q}}_n$ be the position of the particle, at its nth collision, in the infinite horizon Lorentz gas without external fields.*
(a) *We have the following weak convergence, as $n \to \infty$:*

$$\frac{\tilde{\mathbf{q}}_n}{\sqrt{n \log n}} \Rightarrow \mathcal{N}(0, \hat{\mathbf{D}}),$$

*where $\hat{\mathbf{D}}$ will be called discrete-time* superdiffusion matrix.
(b) *The matrix $\hat{\mathbf{D}}$ is non-degenerate iff there are two non-parallel corridors.*

The matrix $\hat{\mathbf{D}}$ is given by a simple explicit formula in terms of the geometric characteristics of the infinite corridors. Namely, suppose that each infinite corridor in $\tilde{\mathcal{D}}$ is bounded by two straight lines, each of which is tangent to an infinite row of scatterers that are copies of a scatterer in $\mathcal{D}$; then such lines are trajectories of some fixed points $X \in \mathcal{M} \colon \mathcal{F}(X) = X$. Now we have

$$\hat{\mathbf{D}} = \sum \frac{c_\nu w_X^2}{2\,\|\boldsymbol{\Delta}(X)\|}\, \boldsymbol{\Delta}(X) \otimes \boldsymbol{\Delta}(X). \tag{2.1}$$

where the sum is over all corridors, $\boldsymbol{\Delta}(X) = \boldsymbol{\Delta}_0(X)$ is the displacement vector of $X$ introduced earlier and $w_X$ is the width of the corridor bounded by the trajectory of $X$.

Our first result is the continuous time version of this theorem, which also includes the Weak Invariance Principle. We remind the reader that the initial position $\tilde{\mathbf{q}}(0)$ and the initial velocity $\mathbf{v}(0)$ are always chosen according to a smooth compact supported distribution.

**Theorem 5.** *Let $\tilde{\mathbf{q}}(t)$ be the position of the particle in the infinite horizon Lorentz gas without external fields.*
(a) *We have the following weak convergence, as $t \to \infty$:*

$$\frac{\tilde{\mathbf{q}}(t)}{\sqrt{t \log t}} \Rightarrow \mathcal{N}(0, \mathbf{D}),$$

*where $\mathbf{D}$ will be called* superdiffusion matrix.
(b) *The latter is $\mathbf{D} = \bar{\tau}_0^{-1} \hat{\mathbf{D}}$, where $\bar{\tau}_0$ is the mean free path given by* (1.4)*. In particular, $\mathbf{D}$ is non-degenerate iff there are two non-parallel corridors.*
(c) *Furthermore, in the latter case (when $\mathbf{D}$ is non-degenerate), we have the Weak Invariance Principle, i.e. the process*

$$\frac{\tilde{\mathbf{q}}(sT)}{\sqrt{T \log T}}, \qquad 0 < s < 1,$$

*converges, as $T \to \infty$, to the Brownian Motion with zero mean and covariance matrix $\mathbf{D}$.*

The case of parallel corridors will be treated separately, see below. In the course of proving Theorem 5 will also provide a different proof of Theorem 4 than the one published in [28].

**Lorentz gas under an external field.** Our main goal is to show that in the 2D periodic Lorentz gas with infinite horizon and a small constant external field $\mathbf{E}$ coupled with a Gaussian thermostat, the electrical current is abnormal, too. Namely if again we denote $\varepsilon = \|\mathbf{E}\|$, then the current $\mathbf{J}$ will be proportional to $\varepsilon |\log \varepsilon|$, rather than $\varepsilon$.

To be precise, there are two distinct cases now. First, if the field $\mathbf{E}$ happens to be parallel to one of the infinite corridors, then with positive probability the particle falls into that corridor and then keeps moving 'ballistically', without collisions. In that case $\tilde{\mathbf{q}}(t)/t$ converges, as $t \to \infty$, to 1 (independently of $\varepsilon$), and this is a trivial case.

A more interesting is a generic situation where the field $\mathbf{E}$ is not parallel to any of the corridors. Now the free paths happen to be bounded, as the particle's trajectory bends under the action of the field and is bound to exit any corridor; see Figure 1. We will actually show that the longest free path between collisions is $\mathcal{O}(\varepsilon^{-1/2})$.

As before, we fix the direction of $\mathbf{E}$ and regard $\varepsilon = \|\mathbf{E}\|$ as a small parameter of the model. Due to the periodicity, we get a flow $\Phi_\varepsilon^t$ on $\Omega = \mathcal{D} \times \mathbb{S}^1$ and a collision map $\mathcal{F}_\varepsilon \colon \mathcal{M} \to \mathcal{M}$. Recall that $\tau = \tau_\varepsilon$ denotes the first collision time (1.2) and $\mathbf{\Delta}_\varepsilon$ denotes the displacement before the first collision (1.6). Our main result is

**Theorem 6.** *Let $\tilde{\mathbf{q}}(t)$ be the position of the particle in the infinite horizon Lorentz gas with a small external field $\mathbf{E}$ coupled with a Gaussian thermostat* (1.5)*. Assume that $\mathbf{E}$ is not parallel to any of the infinite corridors.*
(a) *For small enough $\varepsilon$, the collision map $\mathcal{F}_\varepsilon$ is hyperbolic; it preserves an SRB measure (steady state) $\nu_\varepsilon$, which is ergodic, mixing, and positive on open sets. The flow $\Phi_\varepsilon^t$ also preserves an SRB measure $\mu_\varepsilon$ on $\Omega$, which is ergodic, mixing, and positive on open sets. The electrical current*

$$\mathbf{J} = \lim_{t\to\infty} \tilde{\mathbf{q}}(t)/t = \mu_\varepsilon(\mathbf{v}) = \nu_\varepsilon(\mathbf{\Delta}_\varepsilon)/\bar{\tau}_\varepsilon \tag{2.2}$$

*is well defined; here $\bar{\tau}_\varepsilon = \nu_\varepsilon(\tau_\varepsilon)$ is the mean free path (the average intercollision time).*
(b) *The current $\mathbf{J}$ satisfies*

$$\mathbf{J} = \tfrac{1}{2}\,|\log\varepsilon|\mathbf{D}\mathbf{E} + \delta\mathbf{J}, \tag{2.3}$$

*where $\mathbf{D}$ is the superdiffusion matrix of Theorem 5. The remainder term $\delta\mathbf{J}$ in* (2.3) *is bounded as follows:*

$$\|\delta\mathbf{J}\| \le A_{\mathbf{u}}\varepsilon, \tag{2.4}$$

*where $A_{\mathbf{u}} > 0$ only depends on the direction $\mathbf{u} = \mathbf{E}/\|\mathbf{E}\|$ of the field.*
(c) *We have the following weak convergence, as $t \to \infty$:*

$$\frac{\tilde{\mathbf{q}}(t) - \mathbf{J}t}{\sqrt{t}} \Rightarrow \mathcal{N}(0, \mathbf{D}_\varepsilon), \tag{2.5}$$

*where $\mathbf{D}_\varepsilon$ is the corresponding* diffusion matrix.
(d) *The latter satisfies*

$$\mathbf{D}_\varepsilon = |\log\varepsilon|\,\mathbf{D} + \delta\mathbf{D} \tag{2.6}$$

*where $\|\delta\mathbf{D}\| \le B_{\mathbf{u}}$ is a constant depending on $\mathbf{u}$ only.*

Furthermore, the position process $\{\tilde{\mathbf{q}}(t) - \mathbf{J}t\}$ satisfies the standard Weak Invariance Principle (WIP), Almost Sure Invariance Principle (ASIP), and Law of Iterated Logarithms (LIL), see e.g. [13, Section 7.9].

We remark that the scalars $A_{\mathbf{u}}$ and $B_{\mathbf{u}}$, as functions of $\mathbf{u}$, are not uniformly bounded. In fact we expect that they grow to infinity when the field becomes almost parallel to one of the infinite corridors (this happens because the current $\mathbf{J}$ then seems to be of order one, as we noted above, but we do not investigate this case here).

Theorem 6 suggests that, analogously to (1.10), the position of the particle can be roughly approximated by

$$\tilde{\mathbf{q}}(t) \approx \big[\tfrac{1}{2}\,|\log\varepsilon|\,\mathbf{D} + \mathcal{O}(1)\big]\mathbf{E}\,t + \big[(|\log\varepsilon|\mathbf{D})^{1/2} + \mathcal{O}(1)\big]Z\sqrt{t}, \tag{2.7}$$

where $Z$ denotes the 2D standard normal random vector.

Observe that since the convergence in Theorem 6 is not uniform, (2.7) is only valid for sufficiently large $t$. More precisely we have

**Proposition 2.1.** *Suppose that $t \to \infty$ and $\varepsilon \to 0$. Then*

$$\frac{\tilde{\mathbf{q}}(t) - \mathbf{J}t}{\sqrt{t \log \min\{t, \varepsilon^{-1}\}}} \Rightarrow \mathcal{N}(0, \mathbf{D}).$$

Comparing the finite and infinite horizon cases we make the following observations:

• The classical Ohm's law fails in the infinite horizon case because the electrical conductivity becomes infinite.

• Einstein relation, in the form (1.9), remains valid.

• The continuity of the diffusion matrix loses its meaning since the diffusion matrix (1.3) turns infinite in the absence of fields. Instead, we have the superdiffusion matrix $\mathbf{D}$ that depends on the geometry of the infinite corridors only, and so we observe the following behavior. The field bends the billiard trajectories and caps the longest free path at the level $\mathcal{O}(\varepsilon^{-1/2})$. Such high values of the free path are achieved by typical field-free (billiard) trajectories at times $t \sim \varepsilon^{-1}$. Therefore for $t \ll \varepsilon^{-1}$ the field can be neglected and the effective covariance matrices are about the same, with and without the field. But at larger times, $t \gg \varepsilon^{-1}$, the presence of the field leads to much smaller fluctuations compared to those in the field free case. This explains why we have a diffusion when a field is present and a superdiffusion without fields.

• The superdiffusion matrix $\mathbf{D}$ admits a simple and explicit description in terms of the geometric parameters of the infinite corridors, see (2.1), which is in stark contrast with the diffusion matrix $\mathbf{D}^*$ given by an infinite series (1.3). However, if the scatterers become so small that the number of corridors becomes large, then the evaluation of $\mathbf{D}$ by (2.1) may be also very complicated; see also [21, 22].

**Special case of parallel corridors.** The results of the previous section are valid for any number and configuration of corridors, but they present an incomplete picture when all corridors are parallel, since the matrix $\mathbf{D}$ will be then degenerate. For example, Theorem 5 will only say in this case that typical fluctuations of the particle in the direction perpendicular to the corridors are $o(\sqrt{t \log t})$. On the other hand, it easily follows from [5] that the correct scaling in the Central Limit Theorem in this case is $\sqrt{t}$. Below we present a special theorem tailored for the case of parallel corridors.

For convenience, in this theorem and subsequent propositions the coordinate frame is chosen so that all the infinite corridors are parallel

to the $x$-axis. Note: this is different from our previous convention that the $x$-axis is parallel to the field $\mathbf{E}$. This new choice of the coordinate frame is only adopted within the current subsection, then we return to the old choice where the $x$ direction is parallel to $\mathbf{E}$.

**Theorem 7.** *Let $\tilde{\mathbf{q}}(t) = (x(t), y(t))$ be the position of the particle in the infinite horizon Lorentz gas without external fields, where all the infinite corridors are parallel to the $x$ axis.*
(a) *We have a weak convergence, as $t \to \infty$,*

$$\left( \frac{x(t)}{\sqrt{t \log t}}, \frac{y(t)}{\sqrt{t}} \right) \Rightarrow \mathcal{N}\left(0, \begin{pmatrix} \mathbf{D}_{xx} & 0 \\ 0 & \mathbf{D}^*_{yy} \end{pmatrix}\right).$$

*Here $\mathbf{D}_{xx}$ is the first component of the superdiffusion matrix $\mathbf{D}$ in Theorem 5 and $\mathbf{D}^*_{yy}$ is the last component of the diffusion matrix $\mathbf{D}^*$ in Theorem 1.*
(b) *Furthermore, we have the Weak Invariance Principle, i.e. the process*

$$\left( \frac{x(sT)}{\sqrt{T \log T}}, \frac{y(sT)}{\sqrt{T}} \right), \qquad 0 < s < 1,$$

*converges, as $T \to \infty$, to the Brownian Motion with zero mean and covariance matrix $\begin{pmatrix} \mathbf{D}_{xx} & 0 \\ 0 & \mathbf{D}^*_{yy} \end{pmatrix}$.*

We note that a discrete version of Theorem 7(a) was conjectured in [28, p. 70].

Next we modify Proposition 2.1 in the case where all the corridors are parallel.

**Proposition 2.2.** *Under the assumptions of Theorem 6, suppose that all the corridors are parallel to the $x$ axis. Then the diffusion matrix $\mathbf{D}_\varepsilon$ satisfies*

$$\begin{aligned} (\mathbf{D}_\varepsilon)_{xx} &= |\log \varepsilon| \mathbf{D}_{xx} + \mathcal{O}(1), \\ (\mathbf{D}_\varepsilon)_{xy} &= \mathbf{D}^*_{xy} + o(1), \\ (\mathbf{D}_\varepsilon)_{yy} &= \mathbf{D}^*_{yy} + o(1). \end{aligned}$$

Proposition 2.2 implies that the diffusion matrix $\mathbf{D}_\varepsilon$ has two eigenvalues: the larger is $\sim |\log \varepsilon| \mathbf{D}_{xx}$ and the smaller is $\sim \mathbf{D}^*_{yy}$, and the corresponding eigenvectors are $\mathcal{O}(|\log \varepsilon|^{-1})$-close to the coordinate axes.

**Proposition 2.3.** *Under the assumptions of Theorem 6, suppose that all the corridors are parallel to the $x$ axis. Let $t \to \infty$ and $\varepsilon \to 0$*

*simultaneously. Then*

$$\left( \frac{x(t)}{\sqrt{t \log \min\{t, \varepsilon^{-1}\}}}, \frac{y(t)}{\sqrt{t}} \right) \Rightarrow \mathcal{N}\left(0, \begin{pmatrix} \mathbf{D}_{xx} & 0 \\ 0 & \mathbf{D}^*_{yy} \end{pmatrix}\right).$$

**Related issues.** There is a set of further interesting properties of the Lorentz gas under a small external field with the Gaussian thermostat. For the finite horizon case, they were derived in [11, 12]; for the infinite horizon case, the arguments carry over without change. We list all these results here, referring for the proofs to [11].

First, let $\lambda_\varepsilon^- < 0 < \lambda_\varepsilon^+$ denote the positive and negative Lyapunov exponents of the flow $\Phi_\varepsilon^t$ (it also has one zero Lyapunov exponent). Their sum $\lambda_\varepsilon^+ + \lambda_\varepsilon^-$ represents the average rate of volume contraction under the flow $\Phi^t$. Precisely, if $\dot X = \mathbf{V}(X)$ denote the equations of motion ($X$ stands for the point in the phase space of the flow, $\dot X$ for its time derivative, and $\mathbf{V}(X)$ for the velocity vector field), then

$$\lambda_\varepsilon^+ + \lambda_\varepsilon^- = \mu_\varepsilon\big(\nabla_X \cdot \mathbf{V}(X)\big),$$

where $\nabla_X \cdot \mathbf{V}(X)$ is the divergence of $\mathbf{V}$ see [11, p. 572]. The peculiar feature of our equations of motion (1.5) is that

$$\nabla_X \cdot \mathbf{V}(X) = -\langle \mathbf{E}, \mathbf{v} \rangle,$$

in the notation of (1.5). Therefore

$$\lambda_\varepsilon^+ + \lambda_\varepsilon^- = -\langle \mathbf{E}, \mathbf{J} \rangle.$$

In the context of Theorem 2 (i.e., for finite horizon) we get

$$\lambda_\varepsilon^+ + \lambda_\varepsilon^- = -\tfrac{1}{2}\, \mathbf{E}^T \mathbf{D}^* \mathbf{E} + o(\|\mathbf{E}\|^2), \tag{2.8}$$

and in the context of Theorem 6 (infinite horizon)

$$\lambda_\varepsilon^+ + \lambda_\varepsilon^- = -\tfrac{1}{2}\, \mathbf{E}^T \mathbf{D} \mathbf{E} \big|\log \|\mathbf{E}\|\big| + \mathcal{O}(\|\mathbf{E}\|^2). \tag{2.9}$$

Likewise, let $\hat\lambda_\varepsilon^- < 0 < \hat\lambda_\varepsilon^+$ denote the Lyapunov exponents of the collision map $\mathcal{F}_\varepsilon$. Their sum represents the average rate of volume contraction by the map, i.e.

$$\hat\lambda_\varepsilon^+ + \hat\lambda_\varepsilon^- = \nu_\varepsilon(\ln g),$$

where $g = d\mathcal{F}_\varepsilon^{-1}\nu_0 / d\nu_0$ is the Jacobian of the map $\mathcal{F}_\varepsilon$ with respect to the billiard invariant measure $\nu_0$. Again a direct calculation shows that $g = e^{-\langle \mathbf{E}, \mathbf{\Delta}_\varepsilon \rangle}$, hence

$$\hat\lambda_\varepsilon^+ + \hat\lambda_\varepsilon^- = -\bar\tau_\varepsilon \, \langle \mathbf{E}, \mathbf{J} \rangle.$$

Thus we get

$$\hat\lambda_\varepsilon^+ + \hat\lambda_\varepsilon^- = -\tfrac{1}{2}\, \bar\tau_0 \, \mathbf{E}^T \mathbf{D}^* \mathbf{E} + o(\|\mathbf{E}\|^2) \tag{2.10}$$

for the finite horizon case and

$$\hat\lambda_\varepsilon^+ + \hat\lambda_\varepsilon^- = -\tfrac{1}{2}\,\bar\tau_0\,\mathbf{E}^T\mathbf{D}\mathbf{E}\big|\log\|\mathbf{E}\|\big| + \mathcal{O}(\|\mathbf{E}\|^2) \tag{2.11}$$

for the infinite horizon. We used the fact that $\bar\tau_\varepsilon = \bar\tau_0 + \mathcal{O}(\varepsilon^a)$ for some $a > 0$, which will be proved in Proposition 3.1.

The formulas (2.8)–(2.11) allow us to estimate the fractal (information) dimension (denoted by HD) of the invariant measures $\mu_\varepsilon$ and $\nu_\varepsilon$. First, $\mathrm{HD}(\mu_\varepsilon) = \mathrm{HD}(\nu_\varepsilon) + 1$, and by Young's formula [30]

$$\mathrm{HD}(\nu_\varepsilon) = h_{\nu_\varepsilon}(\mathcal{F}_\varepsilon)\left(\frac{1}{\hat\lambda_\varepsilon^+} - \frac{1}{\hat\lambda_\varepsilon^-}\right),$$

where $h_{\nu_\varepsilon}(\mathcal{F}_\varepsilon)$ is the Kolmogorov-Sinai entropy of the map $\mathcal{F}_\varepsilon$. By Pesin's formula $h_{\nu_\varepsilon}(\mathcal{F}_\varepsilon) = \hat\lambda_\varepsilon^+$. This implies

$$\mathrm{HD}(\mu_\varepsilon) = 2 - \frac{\lambda_\varepsilon^+}{\lambda_\varepsilon^-} = 3 - \frac{\lambda_\varepsilon^+ + \lambda_\varepsilon^-}{\lambda_\varepsilon^-}.$$

Therefore

$$\mathrm{HD}(\mu_\varepsilon) = 3 - \tfrac{\bar\tau_0}{2h_0}\,\mathbf{E}^T\mathbf{D}^*\mathbf{E} + o(\|\mathbf{E}\|^2) \tag{2.12}$$

in the finite horizon case and

$$\mathrm{HD}(\mu_\varepsilon) = 3 - \tfrac{\bar\tau_0}{2h_0}\,\mathbf{E}^T\mathbf{D}\mathbf{E}\big|\log\|\mathbf{E}\|\big| + o\big(\|\mathbf{E}\|^2\big|\log\|\mathbf{E}\|\big|\big) \tag{2.13}$$

in the infinite horizon case. Here $h_0 = h_{\nu_0}(\mathcal{F}_0)$ denotes the Kolmogorov-Sinai entropy of the billiard map $\mathcal{F}_0$, and we used the continuity of $h_{\nu_\varepsilon}(\mathcal{F}_\varepsilon) = \hat\lambda_\varepsilon^+$ at $\varepsilon = 0$; see [11]. We note also that $h_0/\bar\tau_0 = h_{\mu_0}(\Phi^t)$ is the Kolmogorov-Sinai entropy of the billiard flow $\Phi^t$.

Our formulas (2.12)–(2.13) imply that the measure $\mu_\varepsilon$ is singular with respect to the Lebesgue volume for small $\varepsilon \neq 0$, and the same is true for $\nu_\varepsilon$. On the other hand, the support of $\mu_\varepsilon$ is the entire phase space, because every open set has positive measure (Theorem 6); such a situation is common for SRB measures that are obtained by perturbations of a smooth measure, i.e. for non-equilibrium stationary steady states that are close to equilibrium [11, 12].

This completes the statements of our results.

**Structure of the paper.** The paper is organized as follows. In Section 3 we pass to discrete time, i.e. restate our main theorems in terms of the respective collision maps. Then we start proving Theorem 6, which will take seven sections. To help the reader, Section 4 presents a skeleton of our arguments leaving technical calculations for the following six sections. Then in Section 5 we make certain preparations – describe the geometry of trajectories in the infinite corridors and the resulting structure of the collision space $\mathcal{M}$. In Sections 6–7 we review

standard tools for the studies of hyperbolic systems with singularities. In Sections 8–10 we perform the bulk of the technical analysis.

Next, in Section 11 we prove the relatively simpler Theorems 5 and 7. Section 12 contains some technical estimates needed for Section 11, and it concludes with the proofs of Propositions 2.1–2.3.

## 3. Passing to discrete time

It is standard in the studies of continuous time dynamical systems (flows) to convert them to discrete time by using the return map on a suitably constructed cross-section in phase space.

3.1. **Lorentz gas without external forces.** We start with the relatively simpler field-free Lorentz gas. As usual, we represent the continuous time dynamics $\Phi^t\colon \Omega \to \Omega$ by a suspension flow over the collision map $\mathcal{F}\colon \mathcal{M} \to \mathcal{M}$ under the ceiling function $\tau$. Now our Theorems 5 and 7 can be restated for the resulting discrete time process as follows.

**Theorem 8.** *Let $\tilde{\mathbf{q}}_n = (x_n, y_n)$ be the position at the $n$th collision of the particle in the infinite horizon Lorentz gas (without external fields).*
(a) *If there are two non-parallel corridors, then the following Weak Invariance Principle holds: the process*

$$\frac{\tilde{\mathbf{q}}_{sn}}{\sqrt{n\log n}}, \qquad 0 < s < 1,$$

*converges, as $n \to \infty$, to the Brownian Motion with zero mean and covariance matrix $\hat{\mathbf{D}}$ given by* (2.1).
(b) *If all the infinite corridors are parallel (and the coordinate frame is chosen so that the $x$ axis is aligned with the corridors), then the following Weak Invariance Principle holds: the process*

$$\left(\frac{x_{sn}}{\sqrt{n\log n}}, \frac{y_{sn}}{\sqrt{n}}\right), \qquad 0 < s < 1,$$

*converges, as $n \to \infty$, to the Brownian Motion with zero mean and covariance matrix $\begin{pmatrix} \hat{\mathbf{D}}_{xx} & 0 \\ 0 & \hat{\mathbf{D}}^*_{yy} \end{pmatrix}$, where $\hat{\mathbf{D}}^* = \bar{\tau}_0 \mathbf{D}^*$, cf.* (1.3).

Here, as usual, $\tilde{\mathbf{q}}_{sn}$ is a continuous function of $s$ such that $\tilde{\mathbf{q}}_{sn} = \tilde{\mathbf{q}}_m$ whenever $sn = m$ is an integer and obtained by linear interpolation between integers.

Now we can derive Theorems 5 and 7 from Theorem 8. The general results, like [23], do not apply because our functions $\boldsymbol{\Delta}$ and $\tau$ are unbounded and grow rapidly (actually their second moments diverge: $\nu_0(\tau^2) = \nu_0(\|\boldsymbol{\Delta}\|^2) = \infty$), hence we need to provide a problem-specific argument, see next.

In our model, the function $\|\mathbf{\Delta}\| = \tau$ takes large values when the trajectory enters an infinite corridor for a long free flight without collisions. It is known (see [13, Section 4.10] and [28]) that for all $A > 1$

$$\nu_0\big(\tau > A\big) = \mathcal{O}(A^{-2}). \tag{3.1}$$

Now given $T > 0$ and $s \in (0,1)$, let $m_1 = m_1(s,T) = [sT/\bar\tau_0]$ and let $m_2 = m_2(s,T,X)$ be the integer such that $t_{m_2}(X) \le sT < t_{m_2+1}(X)$, where $t_m(X)$ denotes the time of the $m$-th collision. The bound (3.1) implies that

$$\nu_0\Big(\max_{m\le 2T/\bar\tau_0} |t_{m+1} - t_m| \le \sqrt{T}\ln\ln T\Big) \to 1 \tag{3.2}$$

as $T \to \infty$. Note that $\|\tilde{\mathbf{q}}(t') - \tilde{\mathbf{q}}(t'')\| \le |t' - t''|$ because $\|\mathbf{v}(t)\| = 1$. Thus, it suffices to show that

$$\frac{\max_{0<s<1} |\tilde{\mathbf{q}}_{m_1} - \tilde{\mathbf{q}}_{m_2}|}{\sqrt{T\log T}} \to 0$$

in probability. The Ergodic Theorem implies that $t_m(X)/m \to \bar\tau_0$ a.e., as $m \to \infty$. Hence, given $\varepsilon_1, \varepsilon_2 > 0$ we have that for large enough $T$ and for all $s \in (0,1)$

$$\nu_0\big(t_{m_1-\varepsilon_1 T} < sT \quad \text{and} \quad t_{m_1+\varepsilon_1 T} > sT\big) \ge 1 - \varepsilon_2. \tag{3.3}$$

Clearly, (3.2) and (3.3) imply that

$$\nu_0\big(|m_2 - m_1| < \varepsilon_1 T\big) > 1 - 2\varepsilon_2.$$

On the other hand, due to Theorem 8(a) the process $\tilde{\mathbf{q}}_{sT}/\sqrt{T\log T}$ is tight, which means that for any $\varepsilon_1 > 0$ there exists $\varepsilon_2 > 0$ such that if $|m_1 - m_2| < \varepsilon_2 T$, then

$$\nu_0\big(|\tilde{\mathbf{q}}_{m_1} - \tilde{\mathbf{q}}_{m_2}| < \varepsilon_1\sqrt{T\log T}\big) \ge 1 - \varepsilon_1.$$

This implies the Weak Invariance Principle in Theorem 5(c), and the Central Limit Theorem in part (a) immediately follows from (c). The derivation of Theorem 7 from Theorem 8(b) is very similar, and we omit it.

Theorem 8, in turn, is an extension of recent results by Szasz and Varju [28] (Theorem 4); it is proved in Section 11.

3.2. **Lorentz gas under external field.** Now we turn to our main objective – the Lorentz gas under a small external field $\mathbf{E}$. Recall that we fix the direction of $\mathbf{E}$ and regard and $\varepsilon = \|\mathbf{E}\|$ as a small parameter of the model. Again we represent the continuous time dynamics $\Phi_\varepsilon^t \colon \Omega \to$

$\Omega$ by a suspension flow over the collision map $\mathcal{F}_\varepsilon\colon \mathcal{M} \to \mathcal{M}$ under the ceiling function

$$\tau_\varepsilon(X) = \min\{t > 0\colon \Phi_\varepsilon^t(X) \in \mathcal{M}\}.$$

Now Theorem 6 can be restated for the discrete time as follows:

**Theorem 9.** *Let $\tilde{\mathbf{q}}_n$ be the position at the $n$th collision of the particle in the infinite horizon Lorentz gas with a small external field $\mathbf{E}$ coupled with a Gaussian thermostat* (1.5)*. Assume that $\mathbf{E}$ is not parallel to any of the infinite corridors.*
(a) *For small enough $\varepsilon$, the collision map $\mathcal{F}_\varepsilon$ is hyperbolic; it preserves a Sinai-Ruelle-Bowen (SRB) measure (steady state) $\nu_\varepsilon$, which is ergodic, mixing, and positive on open sets. The discrete-time electrical current*

$$\hat{\mathbf{J}} = \lim_{n\to\infty} \tilde{\mathbf{q}}_n/n = \nu_\varepsilon(\mathbf{\Delta}_\varepsilon), \tag{3.4}$$

*is well defined.*
(b) *The current $\hat{\mathbf{J}}$ satisfies*

$$\hat{\mathbf{J}} = \tfrac{1}{2}\,|\log\varepsilon|\hat{\mathbf{D}}\mathbf{E} + \delta\hat{\mathbf{J}}, \tag{3.5}$$

*where*

$$\hat{\mathbf{D}} = \bar{\tau}_0\mathbf{D}, \tag{3.6}$$

*here $\bar{\tau}_0$ is given by* (1.4) *and $\mathbf{D}$ is the matrix of Theorem 5. The remainder term $\delta\hat{\mathbf{J}}$ in* (3.5) *is bounded by:*

$$\|\delta\hat{\mathbf{J}}\| \le \hat{A}_{\mathbf{u}}\varepsilon, \tag{3.7}$$

*where $\hat{A}_{\mathbf{u}} > 0$ only depends on the direction $\mathbf{u} = \mathbf{E}/\|\mathbf{E}\|$ of the field.*
(c) *We have the following weak convergence, as $n \to \infty$:*

$$\frac{\tilde{\mathbf{q}}_n - \hat{\mathbf{J}}n}{\sqrt{n}} \Rightarrow \mathcal{N}(0, \hat{\mathbf{D}}_\varepsilon), \tag{3.8}$$

*where $\hat{\mathbf{D}}_\varepsilon$ is the discrete-time* diffusion matrix*.*
(d) *The latter satisfies*

$$\hat{\mathbf{D}}_\varepsilon = |\log\varepsilon|\,\hat{\mathbf{D}} + \delta\hat{\mathbf{D}} \tag{3.9}$$

*where $\|\delta\hat{\mathbf{D}}\| \le \hat{B}_{\mathbf{u}}$, a constant depending on $\mathbf{u}$ only.*

To derive our main Theorem 6 from Theorem 9, we need the following technical estimate:

**Proposition 3.1.** *The mean free path $\bar{\tau}_\varepsilon = \nu_\varepsilon(\tau_\varepsilon)$ is a Hölder continuous function at $\varepsilon = 0$, i.e.*

$$\left|\bar{\tau}_\varepsilon - \bar{\tau}_0\right| \le \hat{C}_{\mathbf{u}}\varepsilon^a \tag{3.10}$$

*for some constants* $\hat{C}_{\mathbf{u}}, a > 0$*, where* $\hat{C}_{\mathbf{u}}$ *depends on* $\mathbf{u}$ *only.*

Now the derivation of Theorem 6 from Theorem 9 is straightforward. We only note that the continuous time Central Limit Theorem (2.5) follows from its discrete time counterpart (3.8) according to general results, cf. [23] or [13, Theorem 7.68], because (as we will show in Section 5) the functions $\mathbf{\Delta}_\varepsilon$ and $\tau_\varepsilon$ are bounded and regular (more precisely, they are dynamically Hölder continuous, as defined in Section 7).

It remains to prove Theorem 9, and this will be done in the next seven sections.

## 4. Plan of proof of Theorem 9

Here we outline the structure of our arguments leaving the technical calculations for the following six sections.

The map $\mathcal{F}_\varepsilon$ is a small perturbation of the billiard map $\mathcal{F}$, which is known to have strong hyperbolic and ergodic properties. In the case of finite horizon, a perturbative argument was developed in [11, 12, 6, 7] to prove the existence of the SRB measure $\nu_\varepsilon$ and its ergodic and statistical properties, including exponential decay of correlations.

In our case, there is a more serious distinction between $\mathcal{F}_\varepsilon$ and $\mathcal{F}$. The latter has countably many singularity lines which accumulate near fixed points $X \in \mathcal{M}\colon \mathcal{F}(X) = X$ (corresponding to the borders of the infinite corridors; cf. (2.1)). The singularity lines near the fixed points form a characteristic structure of regions (called cells; see e.g. [13, Section 4.10]) which determine global properties of the map $\mathcal{F}$.

Our map $\mathcal{F}_\varepsilon$, on the other hand, has only finitely many singularity lines, and the structure of the corresponding cells is quite different. While our situation is simpler, because of finiteness of the singularity lines, our cells must be carefully analyzed in order to derive properties of $\mathcal{F}_\varepsilon$ similar to those of $\mathcal{F}$. This analysis is done in Section 5; there we will show that $\tau_\varepsilon$ and $\|\mathbf{\Delta}_\varepsilon\|$ are bounded by $\text{const}\cdot\varepsilon^{-1/2}$.

Now the perturbative argument developed in [11, 12, 6, 7] can be used again to construct a unique SRB measure $\nu_\varepsilon$ and prove its ergodic and statistical properties; this will be done in Sections 6–7.

One of the basic properties of the SRB measure $\nu_\varepsilon$ is that it is a weak limit $\nu_\varepsilon = \lim_{n\to\infty} \mathcal{F}_\varepsilon^n \nu_0$. Furthermore, for any smooth function $f$ on

$\mathcal{M}$ we have a Kawasaki-type formula

$$\begin{aligned}\nu_\varepsilon(f) &= \lim_{n\to\infty} \nu_0(f\circ\mathcal{F}_\varepsilon^n)\\ &= \nu_0(f) + \lim_{n\to\infty}\sum_{k=1}^{n} \nu_0\big[(f\circ\mathcal{F}_\varepsilon^k) - (f\circ\mathcal{F}_\varepsilon^{k-1})\big]\\ &= \nu_0(f) + \sum_{k=1}^{\infty} \nu_0\big[(f\circ\mathcal{F}_\varepsilon^k)(1-g)\big], \qquad (4.1)\end{aligned}$$

where

$$g = d\mathcal{F}_\varepsilon^{-1}\nu_0/d\nu_0 = e^{-\langle \mathbf{E},\boldsymbol{\Delta}_\varepsilon\rangle}$$

is the Jacobian of the map $\mathcal{F}_\varepsilon$ with respect to the billiard invariant measure $\nu_0$. We will show that the series in (4.1) converges exponentially fast and uniformly in $\varepsilon$. It is useful to note that $\nu_0(1-g)=0$, because $g$ is the density of a probability measure.

Again, for convenience we choose the coordinate frame so that the direction of the field $\mathbf{E}$ coincides with the positive $x$ axis, then $\mathbf{E} = (\varepsilon, 0)$. Denoting the components of the displacement vector by $\boldsymbol{\Delta}_\varepsilon = (\Delta_{\varepsilon,x}, \Delta_{\varepsilon,y})$ we get

$$g = e^{-\langle \mathbf{E},\boldsymbol{\Delta}_\varepsilon\rangle} = e^{-\varepsilon\Delta_{\varepsilon,x}}. \qquad (4.2)$$

According to (3.4), we need to apply (4.1) to the functions $\Delta_{\varepsilon,x}$ and $\Delta_{\varepsilon,y}$, which are only piecewise-smooth and not uniformly bounded (more precisely, $\sup_{\mathcal{M}}\|\boldsymbol{\Delta}_\varepsilon\| \sim \varepsilon^{-1/2}$). Still, the Kawasaki formula (4.1) applies, and the convergence of the series is uniform in $\varepsilon$; this will be proven in Section 8.

Next we use the invariance of $\nu_\varepsilon$ to write (meaning $\Delta_\varepsilon = \Delta_{\varepsilon,x}$ or $\Delta_{\varepsilon,y}$)

$$\begin{aligned}\nu_\varepsilon(\Delta_\varepsilon) &= \tfrac12\big(\nu_\varepsilon(\Delta_\varepsilon) + \nu_\varepsilon(\Delta_\varepsilon\circ\mathcal{F}_\varepsilon^{-1})\big)\\ &= \tfrac12\big(\nu_0(\Delta_\varepsilon) + \nu_0(\Delta_\varepsilon\circ\mathcal{F}_\varepsilon^{-1})\big) + \sum_{k=1}^{\infty}\nu_0\big[(\Delta_\varepsilon\circ\mathcal{F}_\varepsilon^k)(1-g)\big]\\ &\quad + \tfrac12\nu_0\big[\Delta_\varepsilon\,(1-g)\big]. \qquad (4.3)\end{aligned}$$

Due to the time-reversibility of our dynamics, the first term vanishes, i.e. $\nu_0(\Delta_\varepsilon)+\nu_0(\Delta_\varepsilon\circ\mathcal{F}_\varepsilon^{-1})=0$, see also [11, p. 585]. Next, we use Taylor expansion

$$1-g = \varepsilon\Delta_{\varepsilon,x} + \varepsilon\mathcal{R}_\varepsilon, \qquad (4.4)$$

where $\mathcal{R}_\varepsilon$ denotes the remainder term. We will show in Section 8 that $\mathcal{R}_\varepsilon = \mathcal{O}(1)$ uniformly in $\varepsilon$. Also, $\mathcal{R}_\varepsilon$ has the same degree of regularity

as the function $\Delta_{\varepsilon,x}$ itself, and $\mathcal{R}_\varepsilon \to 0$, as $\varepsilon \to 0$, pointwise. Thus the contribution of $\mathcal{R}_\varepsilon$ will be easy to suppress. Now

$$\sum_{n=1}^{\infty} \nu_0\big[(\Delta_\varepsilon \circ \mathcal{F}_\varepsilon^n)(1-g)\big] = \varepsilon \sum_{n=1}^{\infty} \nu_0\big[(\Delta_\varepsilon \circ \mathcal{F}_\varepsilon^n)(\Delta_{\varepsilon,x} + \mathcal{R}_\varepsilon)\big]. \tag{4.5}$$

On the right-hand side we have the sum of correlation-like terms, which will be shown to be uniformly bounded, thus the left-hand side is $\mathcal{O}(\varepsilon)$. Uniform bounds on correlations constitute our main technical results; they are presented in Section 9.

We now see that the main contribution to the current $\hat{\mathbf{J}}$ comes from the last term in (4.3), which is

$$\nu_0\big[\Delta_\varepsilon(1-g)\big] = \varepsilon\nu_0(\Delta_\varepsilon \Delta_{\varepsilon,x}) + \varepsilon\nu_0(\Delta_\varepsilon \mathcal{R}_\varepsilon).$$

The last term is negligible, as we will show that

$$\nu_0(\Delta_{\varepsilon,x}\mathcal{R}_\varepsilon) = \nu_0(\Delta_{\varepsilon,y}\mathcal{R}_\varepsilon) = \mathcal{O}(\sqrt{\varepsilon}). \tag{4.6}$$

Lastly, we will show, by direct calculation (see Section 10), that

$$\nu_0(\Delta_{\varepsilon,x}^2) = \hat{\mathbf{D}}_{xx} |\log \varepsilon| + \mathcal{O}(1) \tag{4.7}$$

and

$$\nu_0(\Delta_{\varepsilon,x}\Delta_{\varepsilon,y}) = \hat{\mathbf{D}}_{xy} |\log \varepsilon| + \mathcal{O}(1) \tag{4.8}$$

$\hat{\mathbf{D}}_{xx}$ and $\hat{\mathbf{D}}_{xy}$ are the respective components of the superdiffusion matrix $\hat{\mathbf{D}}$ given by (2.1). This will complete our proof of (3.5)–(3.7).

Next we turn to (3.8)–(3.9). The convergence to a normal law $\mathcal{N}(\mathbf{0}, \hat{\mathbf{D}}_\varepsilon)$ is just a central limit theorem proved by standard arguments [5, 6] (which apply because the function $\mathbf{\Delta}_\varepsilon$ is bounded and Hölder continuous). The covariance matrix $\hat{\mathbf{D}}_\varepsilon$ is given by the sum of correlations

$$\hat{\mathbf{D}}_\varepsilon = \sum_{n=-\infty}^{\infty} \Big( \nu_\varepsilon\big[(\mathbf{\Delta}_\varepsilon \circ \mathcal{F}_\varepsilon^n) \otimes \mathbf{\Delta}_\varepsilon\big] - \nu_\varepsilon(\mathbf{\Delta}_\varepsilon) \otimes \nu_\varepsilon(\mathbf{\Delta}_\varepsilon) \Big). \tag{4.9}$$

We will show that the above series, with the exception of its central term $n = 0$, converges exponentially fast and uniformly in $\varepsilon$, and we will show that $\nu_\varepsilon(\mathbf{\Delta}_\varepsilon) = \mathcal{O}(1)$ uniformly in $\varepsilon$. Hence we arrive at

$$\hat{\mathbf{D}}_\varepsilon = \nu_\varepsilon(\mathbf{\Delta}_\varepsilon \otimes \mathbf{\Delta}_\varepsilon) + \mathcal{O}(1).$$

Next we verify that

$$\nu_\varepsilon(\mathbf{\Delta}_\varepsilon \otimes \mathbf{\Delta}_\varepsilon) = \nu_0(\mathbf{\Delta}_\varepsilon \otimes \mathbf{\Delta}_\varepsilon) + \mathcal{O}(1) \tag{4.10}$$

(note that this expression, along with (4.3)–(4.5), implies the Einstein relation between the electrical conductivity and the diffusion matrix).

To this end we apply the Kawasaki-type formula (4.1) to each component of the matrix

$$\mathbf{\Delta}_\varepsilon \otimes \mathbf{\Delta}_\varepsilon = \begin{bmatrix} \Delta_{\varepsilon,x}^2 & \Delta_{\varepsilon,x}\Delta_{\varepsilon,y} \\ \Delta_{\varepsilon,x}\Delta_{\varepsilon,y} & \Delta_{\varepsilon,y}^2 \end{bmatrix}.$$

They are treated similarly, and we only show the formulas for $\Delta_{\varepsilon,x}^2$:

$$\begin{aligned} \nu_\varepsilon(\Delta_{\varepsilon,x}^2) &= \nu_0(\Delta_{\varepsilon,x}^2) + \sum_{k=1}^{\infty} \nu_0\big[(\Delta_{\varepsilon,x}^2 \circ \mathcal{F}_\varepsilon^k)(1-g)\big], \\ &= \nu_0(\Delta_{\varepsilon,x}^2) + \varepsilon \sum_{n=1}^{\infty} \nu_0\big[(\Delta_{\varepsilon,x}^2 \circ \mathcal{F}_\varepsilon^n)(\Delta_{\varepsilon,x} + \mathcal{R}_\varepsilon)\big]. \end{aligned} \tag{4.11}$$

We will prove that the series is bounded by $\varepsilon^{-a}$ for some $a < 1$, hence we obtain (4.10). Now the components of $\nu_0(\mathbf{\Delta}_\varepsilon \otimes \mathbf{\Delta}_\varepsilon)$ have been computed in (4.7)–(4.8), thus we arrive at (3.9). This will complete the proof of Theorem 9.

Lastly, to prove Proposition 3.1 we need to estimate $|\nu_\varepsilon(\tau_\varepsilon) - \nu_0(\tau)|$. We start by applying Kawasaki formula (4.1) to $\tau_\varepsilon$:

$$\nu_\varepsilon(\tau_\varepsilon) = \nu_0(\tau_\varepsilon) + \varepsilon \sum_{k=1}^{\infty} \nu_0\big[(\tau_\varepsilon \circ \mathcal{F}_\varepsilon^k)(\Delta_{\varepsilon,x} + \mathcal{R}_\varepsilon)\big], \tag{4.12}$$

where the series will be shown to converge exponentially and uniformly in $\varepsilon$. Thus it is enough to estimate $\nu_0(|\tau_\varepsilon - \tau|)$, and we will show that

$$\nu_0\big(|\tau_\varepsilon - \tau|\big) = \mathcal{O}(\varepsilon^a), \tag{4.13}$$

for some $a > 0$, which will be done by direct geometric estimation in Section 10.

## 5. Geometric analysis

The equations of motion (1.5) have an explicit solution: since $\|\mathbf{v}\| = 1$, we can put $\mathbf{v} = (\cos\theta, \sin\theta)$, then (1.5) takes form

$$\dot{x} = \cos\theta, \quad \dot{y} = \sin\theta, \quad \dot{\theta} = -\varepsilon \sin\theta \tag{5.1}$$

(where $\dot{x} = dx/dt$, etc.), and its solution is

$$\begin{aligned} x &= x_0 + \frac{1}{\varepsilon} \log \frac{\sin\theta_0}{\sin\theta} \\ y &= y_0 + \frac{\theta_0 - \theta}{\varepsilon} \\ \theta &= 2\arctan\big(c_0 e^{-\varepsilon t}\big) \end{aligned} \tag{5.2}$$

where $c_0 = \tan(\theta_0/2)$ and $(x_0, y_0, \theta_0)$ denote the initial values. When the particle collides with a scatterer, $\theta$ changes according to the rule of specular reflection.

The subsequent results can be derived from (5.2) by direct analytic calculations, but we present a more geometric argument using Wojtkowski's transformation [29]. It is based on a change of variables that transforms curved trajectories (5.2) into straight lines. Let $z = x + iy$ be a complex variable replacing $x$ and $y$ and let us transform $\tilde{\mathcal{D}}$ by the rule

$$z \mapsto w = T(z) = \int e^{-\varepsilon z}\, dz = \frac{1}{\varepsilon}\big[e^{\varepsilon z} - 1\big] \tag{5.3}$$

(the term $-1$ is introduced to keep the origin fixed). In real variables, if we denote $w = u + iv$, this transformation acts as $T(x, y) = (u, v)$, where

$$\begin{aligned} u &= \varepsilon^{-1}\big[e^{\varepsilon x}\cos\varepsilon y - 1\big] \\ v &= \varepsilon^{-1} e^{\varepsilon x}\sin\varepsilon y. \end{aligned} \tag{5.4}$$

One readily checks that in the $uv$ plane the trajectories are straight lines. Furthermore, since the transformation (5.3) is conformal, the specular reflections are mapped into specular reflections. In the new coordinates the particle is moving with a variable speed, but this is irrelevant as we are only interested in the collision map. Thus our problem reduces to a billiard in a new domain, $T(\tilde{\mathcal{D}}) = \mathcal{Q} \subset \mathbb{R}^2$.

The periodic convex scatterers in the $xy$ plane are mapped into scatterers in the $uv$ plane, which are not located periodically and whose size grows with $x$ (due to the $e^{\varepsilon x}$ factor in (5.4)). If $\kappa$ is the curvature of the boundary of a scatterer in the $xy$ plane, then direct calculation shows that the curvature of its image in the $uv$ plane is $e^{-\varepsilon x}\big(\kappa + \mathcal{O}(\varepsilon)\big)$, i.e. it does not change sign for sufficiently small $\varepsilon$; hence the new scatterers are still convex.

Next we examine how an infinite corridor in the $xy$ is transformed on the $uv$ plane. Consider a sequence of identical scatterers forming the 'border' of a corridor, see grey disks in Fig. 2. Each scatterer is obtained by shifting the previous one by a constant vector $(a, b)$ parallel to the corridor; we assume for simplicity that $a \geq 0$ and $b > 0$, as in the figure. Consider a sequence of points $(x_m, y_m)$, $m = 1, 2, \ldots$, related by

$$x_{m+1} = x_m + a, \qquad y_{m+1} = y_m + b.$$

Their images $(u_m, v_m) = T(x_m, y_m)$ are related as follows:

$$\begin{aligned} u_{m+1} &= e^{\varepsilon a}(u_m\cos\varepsilon b - v_m\sin\varepsilon b) + \varepsilon^{-1}(e^{\varepsilon a}\cos\varepsilon b - 1), \\ v_{m+1} &= e^{\varepsilon a}(u_m\sin\varepsilon b + v_m\cos\varepsilon b) + \varepsilon^{-1}e^{\varepsilon a}\sin\varepsilon b \end{aligned} \tag{5.5}$$

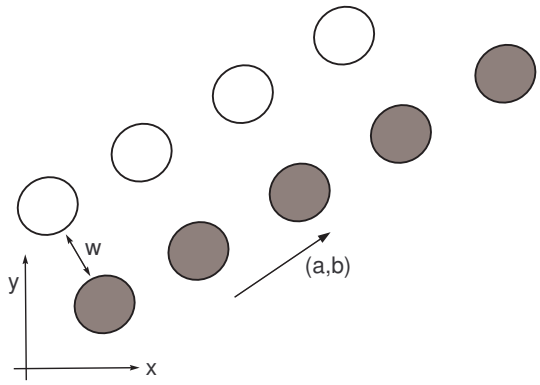


FIGURE 2. A row of scatterers forming the border of an infinite corridor.

This shows that the respective scatterers in the $uv$ plane, see Fig. 3, can be described recursively as follows. Each scatterer $B_{n+1}$ is obtained from the previous one, $B_n$, in three steps:
**1.** $B_n$ is rotated counterclockwise about the origin by angle $\varepsilon b$.
**2.** Then it is expanded homotetically about the origin by factor $e^{\varepsilon a}$.
**3.** Lastly it is shifted by a constant vector

$$(a', b') = \big(\varepsilon^{-1}(e^{\varepsilon a}\cos\varepsilon b - 1), \varepsilon^{-1}e^{\varepsilon a}\sin\varepsilon b\big).$$

This sequence of operations produces the next scatterer $B_{n+1}$ from $B_n$.

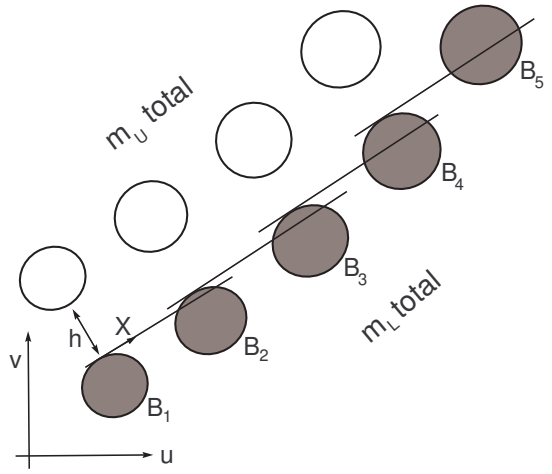


FIGURE 3. The transformed scatterers in the $uv$ plane block the corridor.

Because of rotations, the row of scatterers in the $uv$ plane 'curves up' so the corridor between them is not straight anymore. Only a finite number of scatterers are 'visible' from the neighborhood of the origin, hence the billiard in the new domain $\mathcal{Q}$ has finite horizon. The $m$th scatterer is a distance $\sim cm$ from the origin, where $c = \sqrt{a^2 + b^2}$, hence rotating it by angle $\varepsilon b$ will further block the view along the corridor by the distance $\sim cm\varepsilon b$ in the direction orthogonal to the corridor. The total blockage caused by $m$ scatterers now is

$$cb\varepsilon(1 + 2 + \cdots + m) \sim \tfrac{1}{2}\, cb\varepsilon m^2.$$

If $w$ is the width of the corridor, then the maximal number of scatterers visible from the initial region in the given corridor is $m_{\max} \sim \sqrt{2w/(cb\varepsilon)}$, i.e.

$$m_{\max} \sim C/\sqrt{\varepsilon}. \tag{5.6}$$

We will denote by $C$ various absolute constants (independent of $\varepsilon$) whose values are irrelevant. Note that the growth of the size of the scatterers is negligible – the last visible scatterer is only

$$e^{\varepsilon a m_{\max}} \sim e^{\mathcal{O}(\sqrt{\varepsilon})} \sim 1 + \mathcal{O}(\sqrt{\varepsilon})$$

times larger than the closest one.

Since the billiard in $\mathcal{Q}$ is dispersing and has finite horizon, it has all standard properties [13], in particular uniform expansion and contraction, and a finite number of singularity curves. We note that the expansion in $\mathcal{Q}$ does not automatically imply an expansion in $\tilde{\mathcal{D}}$, because the map $T$ rescales distances (by the factor $e^{\varepsilon x}$), but the maximum rescaling factor in the course of one run between collisions is $e^{\mathcal{O}(\sqrt{\varepsilon})} \approx 1$, hence we still have a uniform expansion for the collision map in the original domain $\tilde{\mathcal{D}}$.

Next we examine the singularity curves of the collision map. Trajectories leaving the initial region into an infinite corridor can land on $\sim m_{\max}$ different scatterers, on either side of the corridor. More precisely, let $m_U$ denote the number of visible scatterers on the upper side of the corridor, and by $m_L$ on the lower side; see Fig. 3. A careful estimation shows that

$$m_U \sim C_1/\sqrt{\varepsilon}, \qquad m_L \sim C_2/\sqrt{\varepsilon}, \qquad 0 < C_1 < C_2$$

thus both $m_U$ and $m_L$ are of order $m_{\max}$. Thus there are $m_U + m_L \sim m_{\max}$ singularity curves. Their number is not uniform, it grows as $\varepsilon \to 0$, thus they require a careful analysis.

Since the trajectories in $\mathcal{Q}$ are straight lines, our analysis goes along the same lines as in billiards with infinite horizon [13, Section 4.10]; it

is standard and elementary and we only present final results. The singularity lines near the point marked by $X$ in Fig. 3 are shown in Fig. 4. The long singularity curve $S$ corresponds to grazing collisions with the very next scatterer in the corridor (marked by $B_2$ in Fig. 3). The short singularity curves are made by grazing collisions with other scatterers in the corridor. The regions between singularity curves are usually called cells, they are made by trajectories landing on a particular scatterer. Thus, the cells can be naturally numbered by $1, \dots, m_U$ (corresponding to the upper scatterers) and $1, \dots, m_L$ (for the lower scatterers). Accordingly, we denote the cells by $D_1^{(U)}, \dots, D_{m_U}^{(U)}$ and $D_1^{(L)}, \dots, D_{m_L}^{(L)}$ (here $U$ and $L$ stand for 'Upper' and 'Lower', respectively).

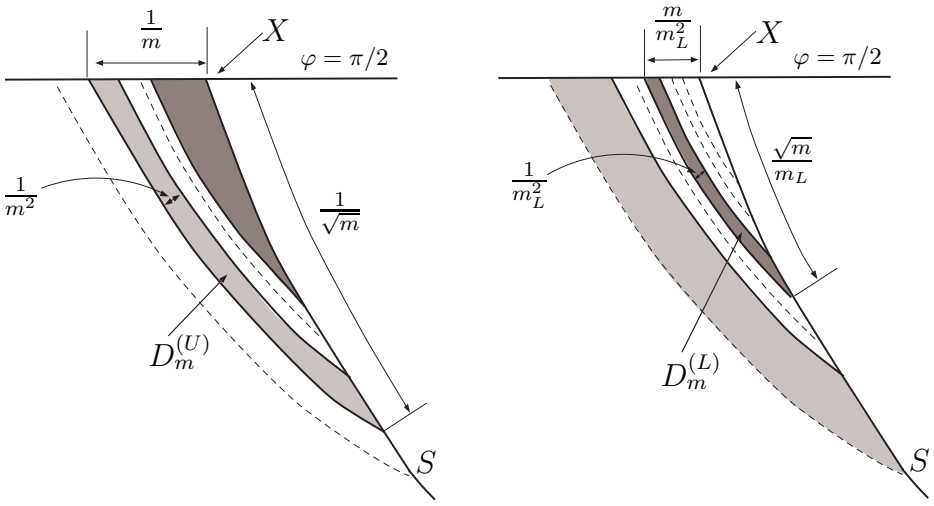


FIGURE 4. Singularity curves and cells. On the left, an 'upper' cell $D_m^{(U)}$ is shown, with all its dimensions, in light grey; the union of all the 'lower' cells $D_m^{(L)}$'s is painted dark grey. On the right, a 'lower' cell $D_m^{(L)}$ is shown, with all its dimensions, in dark grey; the union of all the 'upper' cells $D_m^{(U)}$'s is painted light grey.

In Fig. 4 the cells are depicted as follows. First (farther from $S$) come the cells $D_1^{(U)}, \dots, D_{m_U}^{(U)}$ (in this order). The height of $D_m^{(U)}$ is $\mathcal{O}(1/\sqrt{m})$ and its width is $\mathcal{O}(1/m^2)$, just like in classical billiards with infinite horizon, see e.g. [13, Section 4.10]. Here and in the rest of this section $R = \mathcal{O}(m^a)$ means that $c_1 m^a < R < c_2 m^a$ for some constants $0 < c_1 < c_2 < \infty$. Unstable curves inside $D_m^{(U)}$ are expanded by a factor $\Lambda_m^{(U)} = \mathcal{O}(m^{3/2})$.

Second (closer to $S$) come the cells $D_{m_L}^{(L)}, \dots, D_1^{(L)}$ (in the reverse order; the cell $D_1^{(L)}$ is adjacent to the point $X$). The height of $D_m^{(L)}$ is $\mathcal{O}(\sqrt{m}/m_L)$ and its width is $\mathcal{O}(1/m_L^2)$. Unstable curves inside $D_m^{(L)}$ are expanded by a factor $\Lambda_m^{(L)} = \mathcal{O}(m_L\sqrt{m})$. We note that the collision map $\mathcal{F}_\varepsilon$ transforms each cell $D$ into a similar-looking cell, see Fig. 5, except it expands shorter sides of $D$ and contracts its longer sides, so that the expansion factor can be approximated by

$$\Lambda \sim \frac{\text{height of } D}{\text{width of } D},$$

this relation is standard in the studies of dispersing billiards [13].

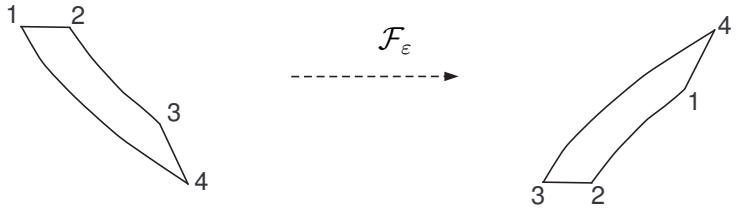


FIGURE 5. The map $\mathcal{F}_\varepsilon$ transforms a cell $D_m^{(U)}$ into a similar-looking domain. The corners of $D_m^{(U)}$ and their respective images are numbered to indicate the action of $\mathcal{F}_\varepsilon$.

We record the following formulas for the measures of the cells:

$$\nu_0\big(D_m^{(U)}\big) = \mathcal{O}(1/m^3), \qquad \nu_0\big(D_m^{(L)}\big) = \mathcal{O}(m/m_L^4). \tag{5.7}$$

Indeed, the billiard measure $\nu_0$ is smooth and has density $\cos\varphi$, thus the measure of each cell is of the same order of magnitude as the product width$\times$(height)$^2$.

## 6. Growth lemmas

Our map $\mathcal{F}_\varepsilon\colon \mathcal{M} \to \mathcal{M}$ is a small perturbation of a dispersing billiard map. The latter enjoys uniformly strong expansion, which is counterbalanced by some mild singularities. The studies of such maps are now well developed, see [11, 5, 6, 7, 8, 9, 14], but there are no axiomatic theory yet that would cover all such models – each new case appears slightly different from others – so we will need to adapt the general arguments to our particular case at some points. We only sketch common steps of this procedure that do not need adaptation, referring to

the original papers for details, and focus on the features novel for our model.

Unstable and stable cones, and respectively unstable and stable curves, for the collision map in dispersing billiards are defined in a standard way [13, Chapter 4]. So we have those objects for the billiard in $\mathcal{Q}$, and transforming them back to $\mathcal{D}$ under $T^{-1}$ gives all such objects for our map $\mathcal{F}_\varepsilon$. Alternatively, unstable curves for $\mathcal{F}_\varepsilon$ can be constructed directly, e.g. by using 'strongly divergent families of flow lines' defined in [6, p. 213].

Next, we may assume as in [6, p. 215] that the curvature of unstable and stable curves is uniformly bounded. To ensure distortion control we construct homogeneity strips in a standard way:

(6.1)
$$\begin{aligned}
\mathbb{H}_j &= \{(r,\varphi)\colon \pi/2 - j^{-2} < \varphi < \pi/2 - (j+1)^{-2}\} \quad \forall j \ge j_0\\
\mathbb{H}_0 &= \{(r,\varphi)\colon \ -\pi/2 + j_0^{-2} < \varphi < \pi/2 - j_0^{-2}\},\\
\mathbb{H}_{-j} &= \{(r,\varphi)\colon \ -\pi/2 + (j+1)^{-2} < \varphi < -\pi/2 + j^{-2}\} \quad \forall j \ge j_0
\end{aligned}$$

where $j_0 > 1$ is a large constant, see [6, p. 216] and [13, Section 5.3]. We cut $\mathcal{M}$ along their boundaries, so that all our stable and unstable curves will be automatically homogeneous. The images and preimages of those boundaries become discontinuity lines (singularities) of $\mathcal{F}_\varepsilon^{-1}$ and $\mathcal{F}_\varepsilon$, respectively. For any unstable curve $W$ and a point $X \in W$ denote by $\mathcal{J}_W\mathcal{F}_\varepsilon^n(X)$ the Jacobian of the map $\mathcal{F}_\varepsilon^n$ restricted to $W$ at $X$. If $\mathcal{F}_\varepsilon^i(W)$ is an unstable curve for all $0 \le i \le n$, then we have the following *distortion bound*, see [6, Lemma 4.2]:

$$|\ln \mathcal{J}_W\mathcal{F}_\varepsilon^n(X) - \ln \mathcal{J}_W\mathcal{F}_\varepsilon^n(Y)| \le C|\mathcal{F}_\varepsilon^n(W)|^{1/3}, \quad X, Y \in W \tag{6.2}$$

where $|W|$ denotes the length of $W$. Accordingly, if $W^u$ is a homogeneous unstable manifold (called h-fiber in [6]) and $\rho_{W^u}$ is the u-SRB density on $W^u$, i.e. the unique probability density satisfying

$$\frac{\rho_{W^u}(X)}{\rho_{W^u}(Y)} = \lim_{n\to\infty} \frac{\mathcal{J}_{W^u}\mathcal{F}_\varepsilon^{-n}(X)}{\mathcal{J}_{W^u}\mathcal{F}_\varepsilon^{-n}(Y)}, \qquad X, Y \in W^u, \tag{6.3}$$

then (6.2) implies $\left|\frac{d}{dX}\ln \rho_{W^u}(X)\right| \le C|W^u|^{-2/3}$; see [13, Section 5.6] and [7].

If $W_1, W_2$ are unstable curves and $\xi$ a stable manifold crossing each $W_i$ in a point $X_i$, then the Jacobian of the holonomy map $\mathbf{h}\colon W_1 \to W_2$ at $X_1$ satisfies

$$e^{-C(\beta+\delta^{1/3})} \le \mathcal{J}\mathbf{h}(X_1) \le e^{-C(\beta+\delta^{1/3})} \tag{6.4}$$

where $\delta = |\xi(X_1, X_2)|$ is the length of the segment of $\xi$ between $X_1$ and $X_2$, and $\beta$ is the angle between the tangent vectors to $W_1$ and $W_2$ at $X_1$ and $X_2$, respectively, see [6, Lemma 4.3], [13, Theorem 5.42], or [7].

The singularity set $\mathcal{S} \subset \mathcal{M}$ of the map $\mathcal{F}_\varepsilon$ is a countable union of stable curves with uniformly bounded curvature. They have the usual 'continuation' and 'alignment' properties, see [13, Chapter 4], i.e. they partition $\mathcal{M}$ into curvilinear polygons with interior angles $< \pi$.

Given $X, Y \in \mathcal{M}$, denote by $\mathbf{s}_+(X, Y) \geq 0$ the future separation time (the first time when the images $\mathcal{F}_\varepsilon^n(X)$ and $\mathcal{F}_\varepsilon^n(Y)$ land on different scatterers or in different homogeneity strips; i.e. the first time when $\mathcal{F}_\varepsilon^{n-1}(X)$ and $\mathcal{F}_\varepsilon^{n-1}(Y)$ belong to different connected components of $\mathcal{M} \setminus \mathcal{S}$), and similarly let $\mathbf{s}_-(X, Y) \geq 0$ denote the past separation time. Observe that if $X$ and $Y$ lie on one unstable curve $W \subset \mathcal{M}$, then $|W(X, Y)| \leq C\Lambda^{-\mathbf{s}_+(X,Y)}$, where $\Lambda > 1$ is the hyperbolicity constant for $\mathcal{F}_\varepsilon$, cf. [13, Eq. (5.32)]. Now (6.4) implies (see, e.g. [13, Proposition 5.48]) that for any $X, Y \in W_1$

$$|\ln \mathcal{J}\mathbf{h}(X) - \ln \mathcal{J}\mathbf{h}(Y)| \leq C\vartheta^{\mathbf{s}_+(X,Y)}, \tag{6.5}$$

where $\vartheta = \Lambda^{-1/6} < 1$. Following Young [31, p. 597], we call the property (6.5) the 'dynamically defined Hölder continuity' of $\mathcal{J}\mathbf{h}$.

Next we derive a key fact about the growth of unstable curves, known as Growth Lemma. Given an unstable curve $W$, let us denote by $W_i \subset W$ the connected components of $W \setminus \mathcal{S}$, i.e. the segments of $W$ on which $\mathcal{F}_\varepsilon$ is smooth, and by $\Lambda_i$ the (minimal) factor of expansion of $W_i$ under $\mathcal{F}_\varepsilon$. Then there is a metric in $\mathcal{M}$, uniformly equivalent to the Euclidean metric $dl^2 = dr^2 + d\varphi^2$, such that

$$\liminf_{\delta_0 \to 0} \sup_{W\colon |W| < \delta_0} \sum_i \Lambda_i^{-1} < 1, \tag{6.6}$$

where the supremum is taken over unstable curves $W$ of length $< \delta_0$. The bound (6.6) is called the one-step expansion estimate [14, Section 5], it shows how much unstable curves stretch under one iteration of the map.

For dispersing billiards with finite horizon, the proof of (6.6) is standard (see [13, Lemma 5.56]), and it readily carries over to perturbed billiards (see [8, Lemma 4.10]) such as systems with small external forces. In our case, infinite corridors add new complications – it is possible that a short unstable curve $W$ intersects many cells described in the previous section (this happens when the images of the pieces $W_i$ move into an infinite corridor and land on different and remote scatterers). Suppose $W$ intersects cells $D_p^{(U)}$, $p_0 \leq p \leq m_U$, and $D_q^{(L)}$,

$q_0 \le q \le m_L$, (the indices are introduced in the previous section), then

$$\sum_i \Lambda_i^{-1} \le \sum_{p=p_0}^{m_U} \frac{C}{p^{3/2}} + \sum_{q=q_0}^{m_L} \frac{C}{m_L q^{1/2}} \le \frac{C}{p_0^{1/2}} + \frac{C}{m_L^{1/2}}.$$

If $W$ is small, then $p_0$ must large, and the above bound is $\ll 1$. This completes the proof of (6.6).

The one-step expansion estimate (6.6) implies several properties known collectively as Growth Lemmas, see [13, Chapter 5], [13, Section 4.7], [6, Proposition 5.3], [8, Lemma 4.10], and the proofs therein. We state their most common version below.

Given an unstable curve $W$, we denote by $m_W$ the Lebesgue measure on it. For every $n \ge 0$, its image $\mathcal{F}_\varepsilon^n(W)$ is a finite or countable union of homogeneous unstable curves called h-components, and for every $X \in W$ we denote by $W_n(X)$ the h-component containing the point $\mathcal{F}_\varepsilon^n(X)$. Now let

$$r_n(X) = r_{W_n(X)}(\mathcal{F}_\varepsilon^n X) \tag{6.7}$$

denote the distance from $\mathcal{F}_\varepsilon^n(X)$ to the nearest endpoint of $W_n(X)$. Clearly, $r_n$ is a function on $W$ that characterizes the size of the h-components of $\mathcal{F}_\varepsilon^n(W)$. We also denote by $\Lambda > 1$ the hyperbolicity constant, i.e. the minimal expansion factor of unstable curves.

**Lemma 6.1** ("Growth lemma"). (a) *There are constants $\vartheta_0 \in (0,1)$ and $c_1, c_2 > 0$, such that for all $n \ge 0$ and $\epsilon > 0$*

$$m_W(r_n(X) < \epsilon) \le c_1(\vartheta_0 \Lambda)^n \, m_W(r_0 < \epsilon/\Lambda^n) + c_2 \epsilon \, m_W(W)$$

(b) *There are constants $c_3, c_4 > 0$, such that if $n \ge c_3 \big|\ln m_W(W)\big|$, then for any $\epsilon > 0$ we have $m_W(r_n(X) < \epsilon) \le c_4 \epsilon \, m_W(W)$.*
(c) *There are constants $\vartheta_1 \in (0,1)$ $c_5, c_6 > 0$, a small $\epsilon_0 > 0$ such that for any $n_2 > n_1 > c_5 \big|\ln m_W(W)\big|$ we have*

$$m_W\Big(\max_{n_1 < n < n_2} r_n(X) < \epsilon_0\Big) \le c_6 \vartheta_1^{n_2 - n_1} m_W(W).$$

For the proof and implications of this lemma we refer to [13, 14]. We emphasize that the lim inf in (6.6) and all the constants in Growth Lemma are independent of $\varepsilon$, i.e. the respective properties hold uniformly in our model parameter $\varepsilon$.

Next we define a class of probability measures supported on unstable curves. A *standard pair* $\ell = (W, \rho)$ is an unstable curve $W \subset \mathcal{M}$ with

a probability measure $\mathbb{P}_\ell$ on it, whose density $\rho$ (with respect to the Lebesgue measure on $W$) satisfies

$$|\ln \rho(X) - \ln \rho(Y)| \le C_{\mathrm{r}}\, \Lambda^{-\mathbf{s}_+(X,Y)}. \tag{6.8}$$

Here $C_{\mathrm{r}} > 0$ is a sufficiently large constant (independent of $\varepsilon$). For any standard pair $\ell = (W, \rho)$ and $n \ge 1$ the image $\mathcal{F}_\varepsilon^n(W)$ is a finite or countable union of h-components on which the density of the measure $\mathcal{F}_\varepsilon^n(\mathbb{P}_\ell)$ satisfies (6.8); hence the image of a standard pair under $\mathcal{F}_\varepsilon^n$ is a family of standard pairs (with a factor measure).

More generally, a *standard family* is an arbitrary (countable or uncountable) collection $\mathcal{G} = \{\ell_\alpha\} = \{(W_\alpha, \rho_\alpha)\}$, $\alpha \in \mathfrak{A}$, of standard pairs with a probability factor measure $\lambda_\mathcal{G}$ on the index set $\mathfrak{A}$. Such a family induces a probability measure $\mathbb{P}_\mathcal{G}$ on the union $\cup_\alpha W_\alpha$ (and thus on $\mathcal{M}$) defined by

$$\mathbb{P}_\mathcal{G}(B) = \int \mathbb{P}_\alpha(B \cap W_\alpha)\, d\lambda_\mathcal{G}(\alpha) \qquad \forall B \subset \mathcal{M}.$$

Any standard family $\mathcal{G}$ is mapped by $\mathcal{F}_\varepsilon^n$ into another standard family $\mathcal{G}_n = \mathcal{F}_\varepsilon^n(\mathcal{G})$, and $\mathbb{P}_{\mathcal{G}_n} = \mathcal{F}_\varepsilon^n(\mathbb{P}_\mathcal{G})$.

For every $\alpha \in \mathfrak{A}$, any point $X \in W_\alpha$ divides the curve $W_\alpha$ into two pieces, and we denote by $r_\mathcal{G}(X)$ the length of the shorter one. Now the quantity $\mathcal{Z}_\mathcal{G} = \sup_{\epsilon>0} \epsilon^{-1} \mathbb{P}_\mathcal{G}(r_\mathcal{G} < \epsilon)$ reflects the 'average' size of curves $W_\alpha$ in $\mathcal{G}$, and we have

$$\mathcal{Z}_\mathcal{G} \le C \int \frac{d\lambda_\mathcal{G}(\alpha)}{|W_\alpha|} \tag{6.9}$$

see [13, Exercise 7.15]. We only consider standard families with $\mathcal{Z}_\mathcal{G} < \infty$. The growth lemma implies that for all $n \ge 0$ and some constant $\theta \in (0, 1)$

$$\mathcal{Z}_{\mathcal{G}_n} \le C(\theta^n \mathcal{Z}_\mathcal{G} + 1), \tag{6.10}$$

see a proof in [13, Proposition 7.17]; this estimate effectively asserts that standard families grow under $\mathcal{F}_\varepsilon^n$ exponentially fast.

A standard pair $(W, \rho)$ is *proper* if $|W| \ge \delta_{\mathrm{p}}$, where $\delta_{\mathrm{p}} > 0$ is a small but fixed constant. A standard family $\mathcal{G}$ is *proper* if $\mathcal{Z}_\mathcal{G} \le C_{\mathrm{p}}$, where $C_{\mathrm{p}}$ is a large but fixed constant (chosen so that a family consisting of a single proper standard pair is proper, as a family). The image of a proper standard family under $\mathcal{F}_\varepsilon^n$ is proper for every $n \ge 1$.

A smooth foliation of $\mathcal{M}$ by (long enough) unstable curves gives us a proper standard family $\mathcal{G}_0$ such that $\mathbb{P}_{\mathcal{G}_0} = \nu_0$, the billiard invariant measure, see [13, p. 172]. Also, there is a special standard family $\mathcal{E}$ consisting of (maximal) unstable manifolds $W^u$ for the map $\mathcal{F}_\varepsilon$ with the SRB densities $\rho_{W^u}$ on them and the factor measure generated by $\nu_\varepsilon$;

in that case $\mathbb{P}_{\mathcal{E}} = \nu_\varepsilon$, the family $\mathcal{E}$ is proper (due to [6, Proposition 5.6]) and obviously $\mathcal{F}_\varepsilon$-invariant.

## 7. Ergodic and statistical properties

Our next task is the existence and uniqueness of the Sinai-Ruelle-Bowen (SRB) measure $\nu_\varepsilon$ on $\mathcal{M}$, which is, by definition, an $\mathcal{F}_\varepsilon$-invariant ergodic measure whose conditional distributions on unstable manifolds are absolutely continuous (and then their conditional densities are given by (6.3)).

The growth lemma can be used to estimate the Lebesgue measure of the $\epsilon$-neighborhood of the singularity set and its pre-images, see details in [6, p. 228], and then standard results, e.g. [25, 26], imply the existence and *finitude* of SRB measures. The finitude means that there are at most finitely many of SRB measures, and each one is mixing and Bernoulli, up to a finite cycle. It also follows from general results that for each SRB measure $\nu$ there is a set $B = B_\nu \subset \mathcal{M}$ of positive Lebesgue measure ('the basin of attraction') such that for every $X \in B$ and any continuous function $f\colon \mathcal{M} \to \mathbb{R}$

$$\frac{1}{n}\big[f(X) + f(TX) + \cdots + f(T^{n-1}X)\big] \to \int_{\mathcal{M}} f(X)\, d\nu$$

as $n \to \infty$, i.e. the SRB measure $\nu$ describes the distribution of randomly selected trajectory with a positive probability; for this reason every SRB measure is said to be physically observable.

The uniqueness and mixing of the SRB measure require a more elaborate argument; it is based on the fact that our map $\mathcal{F}_\varepsilon$ is a small perturbation of a strongly mixing map $\mathcal{F}$ with a smooth invariant measure $\nu_0$. This argument is presented in full detail in [6, pp. 229–233], we only recall its principal steps.

First one finds a domain $R \subset \mathcal{M}$ bounded by two stable and two unstable curves (a curvilinear 'rhombus') such that the images of *every* unstable curve $W \subset \mathcal{M}$ under the billiard map $\mathcal{F}$ cross $R$ fully (intersecting both of its stable sides) at a sufficiently high rate; such an $R$ was constructed in [4], see a more recent account of this construction in [13, Section 7.12]. The growth lemma also guarantees that there are plenty of stable and unstable manifolds crossing the domain $R$ fully, i.e. $R$ is 'saturated' with stable and unstable manifolds.

Then one uses a perturbative argument, see [11, Lemma 13] and [6, p. 230], to extend the above property to the maps $\mathcal{F}_\varepsilon$ with all sufficiently small $\varepsilon$. The rate at which the images of $W$ return to $R$ is bounded below by a constant uniform in $\varepsilon$. Now for any two unstable manifolds $W_1, W_2 \subset \mathcal{M}$ for the map $\mathcal{F}_\varepsilon$ their images under $\mathcal{F}_\varepsilon^n$ for all

sufficiently large $n$ fully cross $R$, hence they can be connected by plenty of stable manifolds of $\mathcal{F}_\varepsilon$. This readily implies the uniqueness and mixing property of the SRB measure $\nu_\varepsilon$, hence its Bernoulli property.

As a side result, the basin of attraction of $\nu_\varepsilon$ has full Lebesgue measure, and due to the mixing property of $\nu_\varepsilon$ we have $\nu_\varepsilon = \lim_{n\to\infty} \mathcal{F}_\varepsilon^n \nu_0$, in the sense of the weak convergence; here $\nu_0$ denotes the $\mathcal{F}$-invariant measure, which has a smooth density, but one can replace $\nu_0$ with any other measure with a smooth positive density on $\mathcal{M}$. An even stronger version of this property will be given shortly.

Now we address the statistical properties of the system $(\mathcal{M}, \mathcal{F}_\varepsilon, \nu_\varepsilon)$. One can use the stable and unstable manifolds that fully cross the rhombus $R$ as a basis for Young's tower and then prove an exponential tail bound for the return times via the growth lemma, as it is done in [5, 14, 16]. This yields exponential decay of correlations.

Alternatively, one can use stable manifolds in $R$ to couple images of unstable curves and prove the so-called coupling lemma, again using the growth lemma as the main tool. This approach is employed in [8, 13, 7, 16]. We state the most important implications of these techniques below.

We say that a function $f\colon \mathcal{M} \to \mathbb{R}$ is *dynamically Hölder continuous* if there are $\vartheta_f \in (0,1)$ and $K_f > 0$ such that for any $X$ and $Y$ lying on one unstable curve

$$|f(X) - f(Y)| \le K_f \vartheta_f^{\mathbf{s}_+(X,Y)} \tag{7.1}$$

and for any $X$ and $Y$ lying on one stable curve

$$|f(X) - f(Y)| \le K_f \vartheta_f^{\mathbf{s}_-(X,Y)}. \tag{7.2}$$

We denote the space of such functions by $\mathcal{H}$. It contains every piecewise Hölder continuous function whose discontinuities coincide with those of $\mathcal{F}_\varepsilon^{\pm m}$ for some $m > 0$. For example, the components $\Delta_{\varepsilon,x}, \Delta_{\varepsilon,y}$ of the vector displacement function $\boldsymbol{\Delta}_\varepsilon$ belong in $\mathcal{H}$ (see the next section).

**Theorem 10** (Equidistribution)**.** *Let $\mathcal{G}$ be a proper standard family. For any dynamically Hölder continuous function $f \in \mathcal{H}$ and $n \ge 0$*

$$\left| \int_{\mathcal{M}} f \circ \mathcal{F}_\varepsilon^n \, d\mathbb{P}_{\mathcal{G}} - \int_{\mathcal{M}} f \, d\nu_\varepsilon \right| \le B_f \theta_f^n \tag{7.3}$$

*where $B_f = 2C\big(K_f + \|f\|_\infty\big)$ and $\theta_f = \big[\max\{\vartheta_1, \vartheta_f\}\big]^{1/2} < 1$; here $C > 0$ and $\vartheta_1 \in (0,1)$ are constants independent of $\mathcal{G}$ and $\varepsilon$.*

In other words, iterations of measures on standard pairs weakly converge to the SRB measure $\nu_\varepsilon$, and the convergence is exponentially fast in the sense of (7.3).

**Theorem 11** (Exponential bound on correlations)**.** *For any pair of dynamically Hölder continuous functions $f, g \in \mathcal{H}$ and $n > 0$*

$$\left|\nu_\varepsilon\big(f \cdot (g \circ \mathcal{F}_\varepsilon^n)\big) - \nu_\varepsilon(f)\nu_\varepsilon(g)\right| \le B_{f,g}\,\theta_{f,g}^n \tag{7.4}$$

*where*

$$\theta_{f,g} = \big[\max\big\{\vartheta_2, \vartheta_f, \vartheta_g\big\}\big]^{1/4} < 1,$$

*(here $\vartheta_2 \in (0,1)$ is a constant independent of $\varepsilon$), and*

$$B_{f,g} = C\big(K_f\|g\|_\infty + K_g\|f\|_\infty + \|f\|_\infty\|g\|_\infty\big).$$

*Remark.* The invariant measure $\nu_\varepsilon$ in (7.4) can be replaced with any measure $\mathbb{P}_\mathcal{G}$ supported on a proper standard family (in particular, by the $\mathcal{F}$-invariant measure $\nu_0$). In that case (7.4) takes form

$$\left|\mathbb{P}_\mathcal{G}\big(f \cdot (g \circ \mathcal{F}_\varepsilon^n)\big) - \mathbb{P}_\mathcal{G}(f)\nu_\varepsilon(g)\right| \le B_{f,g}\,\theta_{f,g}^n.$$

The proof of this is just a simple adaptation of the standard proof of the above theorem, see e.g. the proof of Theorem 3.37 in [13].

The last theorem can be extended to multiple correlations and it implies, via a standard argument, Central Limit Theorem (CLT), Almost Sure Invariance Principle (ASIP), and Law of Iterated Logarithm (LIL) for the map $\mathcal{F}_\varepsilon$, see [13, Chapter 7] and [7]. An argument given in [7, Section 3] also yields the Bernoulli property for the flow $\Phi_\varepsilon^t$, i.e. for the continuous time dynamics of the moving particle in the domain $\mathcal{D}$.

Lastly we derive the Kawasaki-type formula (4.1) for any dynamically Hölder continuous function $f \in \mathcal{H}$. Recall that

$$\nu_\varepsilon(f) = \nu_0(f) + \lim_{n\to\infty} \sum_{k=1}^{n} \nu_0\big[(f \circ \mathcal{F}_\varepsilon^k) - (f \circ \mathcal{F}_\varepsilon^{k-1})\big]. \tag{7.5}$$

Also recall that $\nu_0 = \mathbb{P}_{\mathcal{G}_0}$ for a proper standard family $\mathcal{G}_0$, see the end of Section 6. Thus, due to Equidistribution property (Theorem 10), $\nu_0(f \circ \mathcal{F}_\varepsilon^k)$ converges to $\nu_\varepsilon(f)$ exponentially fast. Therefore the series in (4.1) converges at an exponential rate, and we have the following tail bound:

$$\left|\sum_{k=n}^{\infty} \nu_0\big[(f \circ \mathcal{F}_\varepsilon^k)(1-g)\big]\right| \le 2B_f\theta_f^n/(1-\theta_f). \tag{7.6}$$

We note that if the Hölder exponent $\log\vartheta_f$ of the function $f$, its Hölder norm $K_f$, and its $\infty$-norm $\|f\|_\infty$ are independent of $\varepsilon$, then the above estimate is uniform in $\varepsilon$, too.

## 8. Properties of the $\boldsymbol{\Delta}_\varepsilon$ function

The results in the previous two sections were standard, and so we omitted proofs. From now on our considerations will be quite specific for the model at hand, so we present detailed proofs.

First we estimate the measures of our cells $D_m^{(U)}$ and $D_m^{(L)}$ introduced in Section 5, generalizing (5.7).

**Lemma 8.1.** *For each $n \ge 0$ we have*

$$(\mathcal{F}_\varepsilon^n \nu_0)\big(D_m^{(U)}\big) \sim \frac{C}{m^3}, \qquad (\mathcal{F}_\varepsilon^n \nu_0)\big(D_m^{(L)}\big) \sim \frac{Cm}{m_L^4}. \tag{8.1}$$

*and the same estimates hold for the limit measure $\nu_\varepsilon$.*

*Proof.* For $n = 0$, these were given in (5.7). Recall that the Jacobian of the transformation $\mathcal{F}_\varepsilon$ is $\exp(-\varepsilon\Delta_{\varepsilon,x})$, cf. (4.2), hence the Jacobian of $\mathcal{F}_\varepsilon^n$ is

$$d\mathcal{F}_\varepsilon^{-n}/d\nu_0 = e^{-\varepsilon\sum_{k=0}^{n-1}\Delta_{\varepsilon,x}\circ\mathcal{F}_\varepsilon^k}.$$

Since $\|\Delta_{\varepsilon,x}\|_\infty \le C/\sqrt{\varepsilon}$, due to (5.6), the Jacobian of $\mathcal{F}_\varepsilon^n$ will be, say, in the interval $[0.5, 2]$ for all $n \le c/\sqrt{\varepsilon}$ provided $c > 0$ is a sufficiently small constant. This proves (8.1) for all $n \le c/\sqrt{\varepsilon}$.

For larger $n$'s we use Equidistribution property (Theorem 10); we apply it to the function $f = \mathbf{1}_D$, where $\mathbf{1}_D$ denotes the indicator function of the cell $D = D_m^{(U)}$ or $D = D_m^{(L)}$. Clearly, $f$ is dynamically Hölder continuous with any $\vartheta_f < 1$ and $K_f = 1$, therefore due to (7.3)

$$\big|(\mathcal{F}_\varepsilon^n \nu_0)(D) - \nu_\varepsilon(D)\big| \le C\theta^n$$

for some absolute constants $C > 0$ and $\theta \in (0, 1)$. Now for $n = c/\sqrt{\varepsilon}$ the right hand side is $\theta^{c/\sqrt{\varepsilon}}$, and for all small $\varepsilon$ we have

$$\theta^{c/\sqrt{\varepsilon}} \ll \varepsilon^{3/2} \le \frac{C}{m_U^3} \le \min\left\{\frac{C}{m^3}, \frac{Cm}{m_L^4}\right\},$$

which completes the proof of the lemma. □

Next we verify that the components $\Delta_{\varepsilon,x}$ and $\Delta_{\varepsilon,y}$ of the vector displacement function $\boldsymbol{\Delta}_\varepsilon$ are dynamically Hölder continuous, i.e. belong in $\mathcal{H}$.

**Lemma 8.2.** *Let $X, Y \in \mathcal{M}$ be two nearby points such that their trajectories in $\tilde{\mathcal{D}}$ land, at the next collision, on the same scatterer in $\mathbb{R}^2$. Then we have*

$$\|\boldsymbol{\Delta}_\varepsilon(X) - \boldsymbol{\Delta}_\varepsilon(Y)\| \le C\sqrt{\|\boldsymbol{\Delta}_\varepsilon(X)\| \cdot \operatorname{dist}(X, Y)},$$

*where $C > 0$ is a constant independent of $\varepsilon$.*

*Proof.* Suppose for a moment that we deal with a dispersing billiard with smooth boundary in $\mathbb{R}^2$, i.e. a particle moving between infinitely many smooth convex scatterers whose curvature $\varkappa$ is bounded between two constants,

$$0 < \varkappa_{\min} \le \varkappa \le \varkappa_{\max} < \infty.$$

Let $X = (\mathbf{q}_1, \mathbf{v}_1)$ and $Y = (\mathbf{q}_2, \mathbf{v}_2)$ be two nearby phase points originating from one scatterer such that their images under the collision map land on the same scatterer. By elementary geometry we have

$$\|\mathbf{\Delta}_\varepsilon(X) - \mathbf{\Delta}_\varepsilon(Y)\| \le C\sqrt{\varkappa_{\min}^{-1}\|\mathbf{\Delta}_\varepsilon(X)\| \cdot \operatorname{dist}(X,Y)}.$$

Hence this bound can be applied to the billiard in domain $\mathcal{Q} = T(\tilde{\mathcal{D}})$. It is easy to see that $\varkappa_{\min} \sim e^{-\varepsilon\Delta_{\varepsilon,x}}$, thus the above bound will have a factor $e^{\varepsilon\Delta_{\varepsilon,x}/2}$. But when we transform the images of $X$ and $Y$ back to $\tilde{\mathcal{D}}$, then the distance between them will shrink by a factor of $e^{-\varepsilon\Delta_{\varepsilon,x}}$, which will cancel $e^{\varepsilon\Delta_{\varepsilon,x}/2}$. This proves the lemma. □

Thus the components $\Delta_{\varepsilon,x}, \Delta_{\varepsilon,y}$ of $\mathbf{\Delta}_\varepsilon$ restricted to each cell are Hölder continuous, in the ordinary sense, with Hölder exponent $= 1/2$ and Hölder norm

$$K_\varepsilon = \max_{X\in\mathcal{M}} \|\mathbf{\Delta}_\varepsilon(X)\| \sim C/\sqrt{\varepsilon},$$

see (5.6). This implies that $\Delta_{\varepsilon,x}, \Delta_{\varepsilon,y}$ belong in $\mathcal{H}$, with a fixed value of the parameter $\vartheta_\Delta < 1$ (independent of $\varepsilon$), and with $K_\Delta \sim 1/\sqrt{\varepsilon}$. We note also that

$$\|\Delta_{\varepsilon,x}\|_\infty \sim \|\Delta_{\varepsilon,y}\|_\infty \sim 1/\sqrt{\varepsilon}.$$

Thus the Kawasaki-type formulas (7.5)–(7.6) apply and give

$$\left| \int_{\mathcal{M}} \Delta \circ \mathcal{F}_\varepsilon^n \, d\nu_0 - \int_{\mathcal{M}} \Delta \, d\nu_\varepsilon \right| \le C\varepsilon^{-1/2}\theta^n, \tag{8.2}$$

where $\Delta$ is a shorthand notation for $\Delta_{\varepsilon,x}$ and $\Delta_{\varepsilon,y}$. Furthermore, for every $k \ge 2$ we have $\|\Delta^k\| \sim \varepsilon^{-k/2}$ and

$$\left| \int_{\mathcal{M}} \Delta^k \circ \mathcal{F}_\varepsilon^n \, d\nu_0 - \int_{\mathcal{M}} \Delta^k \, d\nu_\varepsilon \right| \le C\varepsilon^{-k/2}\theta^n. \tag{8.3}$$

For $k = 1$, we can get a uniform bound, independent of $\varepsilon$:

**Proposition 8.3.** *For some constants $C > 0$ and $\theta < 1$, independent of $\varepsilon$,*

$$\left| \int_{\mathcal{M}} \Delta \circ \mathcal{F}_\varepsilon^n \, d\nu_0 - \int_{\mathcal{M}} \Delta \, d\nu_\varepsilon \right| \le C\theta^n, \tag{8.4}$$

*where $\Delta$ is a shorthand notation for $\Delta_{\varepsilon,x}$ and $\Delta_{\varepsilon,y}$.*

*Proof.* Define $\Delta' = \Delta \cdot \mathbf{1}_{\{|\Delta|<H\}}$ and $\Delta'' = \Delta - \Delta'$, where $H$ a certain 'cut-off' value to be selected below. Applying our previous analysis to $\Delta'$ shows that the latter is dynamically Hölder continuous with parameters $\vartheta_\Delta < 1$ (uniform in $\varepsilon$) and $K_H \sim H$. Thus (7.3) implies

$$\left| \int_{\mathcal{M}} \Delta' \circ \mathcal{F}_\varepsilon^n \, d\nu_0 - \int_{\mathcal{M}} \Delta' \, d\nu_\varepsilon \right| \le CH\theta^n \tag{8.5}$$

for some absolute constants $C > 0$ and $\theta < 1$.

Now for every $n \ge 0$ we have

$$\left| \int_{\mathcal{M}} \Delta'' \circ \mathcal{F}_\varepsilon^n \, d\nu_0 \right| \le \frac{C}{H}, \tag{8.6}$$

see below. Taking the limit $n \to \infty$ gives $\left|\int_{\mathcal{M}} \Delta'' d\nu_\varepsilon\right| \le C/H$, and thus

$$\left| \int_{\mathcal{M}} \Delta'' \circ \mathcal{F}_\varepsilon^n \, d\nu_0 - \int_{\mathcal{M}} \Delta'' \, d\nu_\varepsilon \right| \le \frac{2C}{H}. \tag{8.7}$$

To prove (8.6) note that $\Delta \sim Cm$ on every cell $D_m^{(U)}$ (see Section 5) for some $C > 0$, and using the first estimate in (8.1) we get the sum

$$\sum_{m=H/C}^{m_U} \frac{Cm}{m^3} \sim \frac{C}{H}.$$

Similarly, $\Delta \sim Cm$ on every cell $D_m^{(L)}$, and using the second estimate in (8.1) we get the sum

$$\sum_{m=H/C}^{m_L} \frac{Cm^2}{m_L^4} \le \frac{C}{m_L} \le \frac{C}{H}$$

in the case $H < Cm_L$, and otherwise the sum is vacuous.

Combining (8.5) and (8.7) gives, for some $C > 0$,

$$\left| \int_{\mathcal{M}} \Delta \circ \mathcal{F}_\varepsilon^n \, d\nu_0 - \int_{\mathcal{M}} \Delta \, d\nu_\varepsilon \right| \le C(H\theta^n + 1/H).$$

Now choosing $H = \theta^{-n/2}$ produces the desired uniform tail bound (8.4). □

We conclude this section by examining the 'remainder' function introduced in (4.4):

$$\mathcal{R}_\varepsilon = \frac{1 - e^{-\varepsilon\Delta_{\varepsilon,x}} - \varepsilon\Delta_{\varepsilon,x}}{\varepsilon} = \sum_{k=1}^{\infty} \frac{(-1)^k}{(k+1)!} \, \varepsilon^k \Delta_{\varepsilon,x}^{k+1}. \tag{8.8}$$

One can easily see that $\mathcal{R}_\varepsilon$ is dynamically Hölder continuous with the same characteristics $\vartheta_{\mathcal{R}_\varepsilon} = \vartheta_\Delta$ and $K_{\mathcal{R}_\varepsilon} = K_\Delta$ as the function $\Delta_{\varepsilon,x}$.

On the other hand, since $|\Delta_{\varepsilon,x}| = \mathcal{O}(\varepsilon^{-1/2})$, the function $\mathcal{R}_\varepsilon$ is bounded (uniformly in $\varepsilon$), i.e.

$$|\mathcal{R}_\varepsilon| \le C \tag{8.9}$$

Also, $\mathcal{R}_\varepsilon \to 0$ pointwise, as $\varepsilon \to 0$, see [11, p. 585]. For all these reasons its contribution to (4.5) will be much easier to handle than that of $\Delta_{\varepsilon,x}$, hence we will first focus on the main sum

$$\sum_{k=1}^{\infty} \nu_0\big[(\Delta \circ \mathcal{F}_\varepsilon^k)\Delta_{\varepsilon,x}\big] \tag{8.10}$$

in (4.5), and then adapt our arguments to $\mathcal{R}_\varepsilon$. The sum (8.10) consists of correlation-like terms, which will be analyzed in the next section.

## 9. Correlation bounds

We rewrite (8.10) as

$$\sum_{n=1}^{\infty} \nu_0\big[(\Delta_\varepsilon \circ \mathcal{F}_\varepsilon^n)\Delta_\varepsilon\big] \tag{9.1}$$

where each $\Delta_\varepsilon$ can be replaced with either $\Delta_{\varepsilon,x}$ or $\Delta_{\varepsilon,y}$, and our estimates in this section will apply to all four combinations (though we only deal with two in (4.5)). Also, $\Delta_0$ will mean the displacement when $\varepsilon = 0$, i.e. under the field-free (billiard) dynamics (recall that $\Delta_0$ is truly unbounded).

The sum (9.1) contains correlation-like terms, but they are not exactly correlations, as the measure $\nu_0$ is not $\mathcal{F}_\varepsilon$-invariant. To clarify our ideas, first we bound true correlations for the billiard displacement function $\Delta_0$, which is a new result by itself (it is related to the recent studies in [28], but it is not stated or used there).

**Proposition 9.1.** *For some constants $C > 0$ and $\theta \in (0,1)$ and all $n \ge 1$*

$$\Big|\nu_0\big[(\Delta_0 \circ \mathcal{F}^n)\Delta_0\big]\Big| \le C\theta^n, \tag{9.2}$$

*where each $\Delta_0$ can be replaced with either $\Delta_{0,x}$ or $\Delta_{0,y}$ (under the billiard map $\mathcal{F}$). Note that the restriction $n \ge 1$ is essential here, as $\nu_0(\Delta_0^2) = \infty$.*

*Proof.* The collision space $\mathcal{M}$ is divided by the singularity curves of the map $\mathcal{F}$ into cells $D_m$, such that $\Delta_0 \sim Cm$ on $D_m$. Their measures are $\nu_0(D_m) \sim C/m^3$, their dimensions are $\sim C/\sqrt{m}$ in the stable direction and $\sim C/m^2$ in the unstable direction (just like the 'upper' cells $D_m^{(U)}$ in our case); these are all standard facts [13, 14, 15, 28].

Just like in the previous section, let $\Delta_0' = \Delta_0 \cdot \mathbf{1}_{\{|\Delta_0|<H\}}$ and $\Delta_0'' = \Delta_0 - \Delta_0'$, where $H$ a certain 'cut-off' value to be selected below. We also put $\Delta_0''' = \Delta_0 \cdot \mathbf{1}_{\{|\Delta_0|<H^3\}}$ and $\Delta_0'''' = \Delta_0 - \Delta_0'''$. As we have shown before, $\Delta_0'$ and $\Delta_0'''$ are dynamically Hölder continuous with parameters $\vartheta_\Delta < 1$ and $K_H = \mathcal{O}(H)$ and $K_{H^3} = \mathcal{O}(H^3)$, respectively. Thus the standard bound on correlations [13, Section 7.7] implies

$$\big|\nu_0\big[(\Delta_0''' \circ \mathcal{F}^n)\Delta_0'\big]\big| \le CH^4\theta^n \tag{9.3}$$

for some $C > 0$ and $\theta < 1$ (we note that to the time-reversibility of our dynamics, $\nu_0(\Delta_0) = \nu_0(\Delta_0') = \nu_0(\Delta_0'') = 0$). Next we have

$$\begin{aligned}\big|\nu_0\big[(\Delta_0'''' \circ \mathcal{F}^n)\Delta_0'\big]\big| &\le C\sum_{m=1}^{H}\sum_{k=H^3}^{\infty} mk\nu_0\big[D_m \cap \mathcal{F}^{-n}(D_k)\big]\\ &\le C\sum_{m=1}^{H}\sum_{k=H^3}^{\infty} mk/k^3\\ &\le C/H. \qquad (9.4)\end{aligned}$$

It remains to estimate the quantity

$$\mathcal{A}\colon = \big|\nu_0\big[(\Delta_0 \circ \mathcal{F}^n)\Delta_0''\big]\big| \le C\sum_{m=H}^{\infty}\sum_{k=1}^{\infty} mk\nu_0\big[D_m \cap \mathcal{F}^{-n}(D_k)\big]. \tag{9.5}$$

To estimate the measure $\nu_0\big[D_m \cap \mathcal{F}^{-n}(D_k)\big]$ we foliate $D_m$ by unstable curves $W \subset D_m$; they have length $\sim C/m^2$. The image $\mathcal{F}(D_m)$ is a domain of length $\sim Cm^{-1/2}$ in the unstable direction adjacent to the line $\varphi = \pm\pi/2$ bounding the space $\mathcal{M}$ (see e.g. [13, Section 4.10]). Thus the curves $\mathcal{F}(W)$ are divided into pieces by the boundaries of the homogeneity strips (6.1); those pieces have lengths $\sim 1/j^3$ for $j \ge Cm^{1/4}$, and their pre-images on $W$ have lengths $\sim 1/(mj^5)$, because these pieces are contracted under the map $\mathcal{F}^{-1}$ by a factor $\sim mj^2$. The curve $W$ equipped with the conditional density $\rho$ induced by $\nu_0$ is a standard pair $\ell = (W, \rho)$, and its image $\mathcal{F}(W)$ equipped with the induced measure is a standard family, $\mathcal{G}_{\ell,1}$, whose $\mathcal{Z}$-value (6.9) is

$$\mathcal{Z}_{\mathcal{G}_{\ell,1}} \le C\sum_{j=Cm^{1/4}}^{\infty}\frac{m^2j^3}{mj^5} \le Cm^{3/4}.$$

As this applies to every curve $W$ in our foliation of $D_m$, the measure $\nu_0$ conditioned on $D_m$ is represented by a measure $\mathbb{P}_{\mathcal{G}}$ on the corresponding standard family $\mathcal{G}$, for whose image $\mathcal{G}_1 = \mathcal{F}(\mathcal{G})$ we have $\mathcal{Z}_{\mathcal{G}_1} = \mathcal{O}(m^{3/4})$. Due to (6.10) we also have $\mathcal{Z}_{\mathcal{G}_n} \le Cm^{3/4}$ for all $n \ge 1$. Since each cell

$D_k$ has length $\sim Ck^{-2}$ in the unstable direction, we have

$$\nu_0\big[D_m \cap \mathcal{F}^{-n}(D_k)\big] \le C\nu_0(D_m)\mathcal{Z}_{\mathcal{G}_n}k^{-2} \le Cm^{-9/4}k^{-2}. \tag{9.6}$$

We also have

$$\nu_0\big[D_m \cap \mathcal{F}^{-n}(D_k)\big] \le \nu_0(D_k) = Ck^{-3}. \tag{9.7}$$

Combining (9.6) and (9.7) we estimate (9.5) as follows:

$$\begin{aligned}\mathcal{A} &\le C\sum_{m=H}^{\infty}\sum_{k=1}^{m^3} mkm^{-9/4}k^{-2} + C\sum_{m=H}^{\infty}\sum_{k=m^3}^{\infty} mkk^{-3}\\ &\le C\sum_{m=H}^{\infty} m^{-5/4}\ln m + C\sum_{m=H}^{\infty} mm^{-3}\\ &\le C/H^{1/5}. \qquad (9.8)\end{aligned}$$

Now collecting our estimates (9.3), (9.4), (9.8), and choosing $H = \theta^{-n/5}$ (to suppress the factor $H^4$ in (9.3)) proves Proposition 9.1. □

The main difficulties in the proof are caused by the unboundedness of the function $\Delta_0$. If we replace it by a bounded version

$$\Delta_0^{(H)} = \Delta_0 \cdot \mathbf{1}_{\{|\Delta_0|<H\}}, \tag{9.9}$$

then the proof can be easily modified and we obtain the following:

**Corollary 9.2.** *For some constants $C > 0$ and $\theta \in (0,1)$ and all $n \ge 1$*

$$\Big|\nu_0\big[(\Delta_0^{(H_1)} \circ \mathcal{F}^n)\Delta_0^{(H_2)}\big]\Big| \le C\theta^n, \tag{9.10}$$

We note again that to the time-reversibility of our dynamics

$$\nu_0\big(\Delta_0^{(H)}\big) = 0 \tag{9.11}$$

for any $H > 0$. The bound (9.10) fails for $n = 0$. In fact we have

$$\nu_0\big(\big[\Delta_0^{(H)}\big]^2\big) = \mathcal{O}\bigg(\sum_{m=1}^{H}\frac{m^2}{m^3}\bigg) = \mathcal{O}(\ln H). \tag{9.12}$$

Next we extend Proposition 9.1 to the perturbed map $\mathcal{F}_\varepsilon$:

**Proposition 9.3.** *For some constants $C > 0$ and $\theta \in (0,1)$ independent of $\varepsilon$ and all $n \ge 1$*

$$\Big|\nu_\varepsilon\big[(\Delta_\varepsilon \circ \mathcal{F}_\varepsilon^n)\tilde\Delta_\varepsilon\big] - \nu_\varepsilon(\Delta_\varepsilon)\nu_\varepsilon(\tilde\Delta_\varepsilon)\Big| \le C\theta^n \tag{9.13}$$

*and*

$$\Big|\nu_0\big[(\Delta_\varepsilon \circ \mathcal{F}_\varepsilon^n)\tilde\Delta_\varepsilon\big] - \nu_\varepsilon(\Delta_\varepsilon)\nu_0(\tilde\Delta_\varepsilon)\Big| \le C\theta^n \tag{9.14}$$

*where each of $\Delta_\varepsilon$ and $\tilde\Delta_\varepsilon$ can be replaced with either $\Delta_{\varepsilon,x}$ or $\Delta_{\varepsilon,y}$.*

*Proof.* The proof of (9.13) is very similar to that of Proposition 9.1. The 'upper' cells $D_m^{(U)}$ have shape, size, and $\nu_\varepsilon$-measure given by the same formulas as those of the cells $D_m$ in the field-free Lorentz gas. There are now 'lowers' cells $D_m^{(L)}$ whose characteristics can be computed directly, and then one can follow the lines of the proof of Proposition 9.1, it is straightforward, albeit quite involved, so we omit details.

One can also convince oneself that our argument works by making the following observation. The 'lower' cells $D_m^{(L)}$ are located in the place in $\mathcal{M}$ where the ordinary cells $D_k$ for the field-free Lorentz gas are, compare our Figure 4 with Figure 4.15 in [13]; except our 'lower' cells are thicker. They are also mapped by $\mathcal{F}_\varepsilon$ in the same way as the ordinary cells $D_k$ are mapped by $\mathcal{F}$, compare our Figure 5 with Figure 4.16 in [13]. Thus we can refine the 'lower' cells $D_m^{(L)}$ replacing each one with a union of thinner domains shaped as ordinary cells $D_k$ (as one can see, $k$ should take values $m_L^2/m \le k < m_L^2/(m-1)$, and the last cell $D_1^{(L)}$ will be replaced with a countable union of $D_k$'s with all $k \ge m_L^2$). We can also redefine the map $\mathcal{F}_\varepsilon$ on $D_m^{(L)}$ so that it acts as $\mathcal{F}$ on the corresponding $D_k$'s. Then our analysis of the curves $W$ foliating $D_k$'s (and thus also foliating $D_m^{(L)}$'s will apply, and we will have similar estimates on the $\mathcal{Z}$-values as in the proof of Proposition 9.1. The only substantial difference is that our observables $\Delta_\varepsilon$ are substantially smaller than $\Delta_0$, because $\Delta_\varepsilon \sim m$ on $D_m^{(L)}$, while $\Delta_0 \sim k$ on the 'replacement' cells $D_k$, and $k \gg m$. Thus our observables $\Delta_\varepsilon$ cause much less trouble than $\Delta_0$, and all the bounds established in the proof of Proposition 9.1 will remain valid.

Next we turn to the proof of (9.14). Since the measure $\nu_0$ is not $\mathcal{F}_\varepsilon$-invariant, we first need to apply the remark after Theorem 11, and then repeat the above proof of (9.13). □

We now return to (4.5). Due to Proposition 8.3 (see also (7.5)–(7.6)), the series (4.5) converges exponentially fast and uniformly in $\varepsilon$, hence

$$\left| \sum_{n=L|\log\varepsilon|}^{\infty} \nu_0\big[(\Delta \circ \mathcal{F}_\varepsilon^n)(1-g)\big] \right| = \mathcal{O}(\varepsilon^2)$$

for a sufficiently large $L > 0$, so it remains to handle $n < L|\log\varepsilon|$. Next we will deal with the series on the right hand side of (4.5), i.e. we split off the factor of $\varepsilon$.

The values of $\nu_0\big[(\Delta_\varepsilon \circ \mathcal{F}_\varepsilon^n)\Delta_\varepsilon\big]$ in (9.1) can be estimates by (9.14) in Proposition 9.3:

$$\nu_0\big[(\Delta_\varepsilon \circ \mathcal{F}_\varepsilon^n)\Delta_\varepsilon\big] = \nu_0(\Delta_\varepsilon)\nu_\varepsilon(\Delta_\varepsilon) + \mathcal{O}(\theta^n) \tag{9.15}$$

and similarly, replacing one $\Delta_\varepsilon$ with a much milder function $\mathcal{R}_\varepsilon$ we get

$$\nu_0\big[(\Delta_\varepsilon \circ \mathcal{F}_\varepsilon^n)\mathcal{R}_\varepsilon\big] = \nu_0(\mathcal{R}_\varepsilon)\nu_\varepsilon(\Delta_\varepsilon) + \mathcal{O}(\theta^n) \tag{9.16}$$

(it may seem strange that we approximate terms of the convergent series (9.1) by two non-zero constants, but in fact

$$\nu_0(\Delta_\varepsilon)\nu_\varepsilon(\Delta_\varepsilon) + \nu_0(\mathcal{R}_\varepsilon)\nu_\varepsilon(\Delta_\varepsilon) = 0$$

which follows from the relation $\nu_0(1-g) = 0$, cf. Section 4). Now the contribution of all the $\mathcal{O}(\theta^n)$ terms in (9.15)–(9.16) to the sum (4.5) will total to $\mathcal{O}(\varepsilon)$, which is acceptable. But the contribution of $\nu_0(\Delta_\varepsilon)\nu_\varepsilon(\Delta_\varepsilon)$ and $\nu_0(\mathcal{R}_\varepsilon)\nu_\varepsilon(\Delta_\varepsilon)$ cannot be directly assessed as it contains the unknown quantity $\nu_\varepsilon(\Delta_\varepsilon)$. To bypass this complication we observe that

$$\nu_0(\Delta_\varepsilon) = \mathcal{O}\Big(\sum_{m=1}^{m_U} \frac{m}{m^3}\Big) + \mathcal{O}\Big(\sum_{m=1}^{m_L} \frac{m^2}{m_L^4}\Big) = \mathcal{O}(1).$$

(In fact, we believe that a more careful estimation would produce $\nu_0(\Delta_\varepsilon) = \mathcal{O}(\sqrt{\varepsilon})$, but we will not need it here.) Next, $\nu_0(\mathcal{R}_\varepsilon) = \mathcal{O}(1)$, since $\mathcal{R}_\varepsilon$ is uniformly bounded due to (8.9). Thus we can rewrite (4.3) and (4.5) as

$$\begin{aligned}\nu_\varepsilon(\Delta_\varepsilon) &= \tfrac{1}{2}\nu_0\big[\Delta_\varepsilon\,(1-g)\big] \\ &\quad + L\varepsilon\log|\varepsilon|\big(\nu_0(\Delta_\varepsilon) + \nu_0(\mathcal{R}_\varepsilon)\big)\nu_\varepsilon(\Delta_\varepsilon) + \mathcal{O}(\varepsilon).\end{aligned}$$

Solving this equation for $\nu_\varepsilon(\Delta_\varepsilon)$ gives

$$\nu_\varepsilon(\Delta_\varepsilon) = \tfrac{1}{2}\nu_0\big[\Delta_\varepsilon\,(1-g)\big]\big(1 + \mathcal{O}(\varepsilon\log|\varepsilon|)\big) + \mathcal{O}(\varepsilon). \tag{9.17}$$

It remains to compute $\nu_0\big[\Delta_\varepsilon\,(1-g)\big]$ and prove Proposition 3.1, which will be done in the next section.

## 10. Finishing the proof of Theorem 9

Here we prove the remaining formulas (4.6)–(4.8) and (4.13).

To verify (4.6) we note that for any $k \geq 1$

$$\nu_0\big(\Delta_{\varepsilon,x}^{k+2}\big) = \mathcal{O}\Big(\sum_{m=1}^{m_U} \frac{m^{k+2}}{m^3}\Big) + \mathcal{O}\Big(\sum_{m=1}^{m_L} \frac{m^{k+3}}{m_L^4}\Big) = \mathcal{O}\big(\varepsilon^{-\frac{k}{2}}\big).$$

Then using the series (8.8) gives

$$\nu_0(\Delta_{\varepsilon,x}\mathcal{R}_\varepsilon) = \mathcal{O}\Big(\sum_{k=1}^{\infty} \frac{\varepsilon^{k/2}}{(k+1)!}\Big) = \mathcal{O}\big(\varepsilon^{1/2}\big). \tag{10.1}$$

As for (4.7), we have

$$\nu_0(\Delta_{\varepsilon,x}^2) = \mathcal{O}\Big(\sum_{m=1}^{m_U} \frac{m^2}{m^3}\Big) + \mathcal{O}\Big(\sum_{m=1}^{m_L} \frac{m^3}{m_L^4}\Big) = \mathcal{O}\big(|\log\varepsilon|\big) + \mathcal{O}(1), \tag{10.2}$$

and a similar estimate readily applies to $\nu_0(\Delta_{\varepsilon,x}\Delta_{\varepsilon,y})$. To obtain a more precise asymptotics claimed in (4.7)–(4.8) we need to return to the geometric analysis of Section 5.

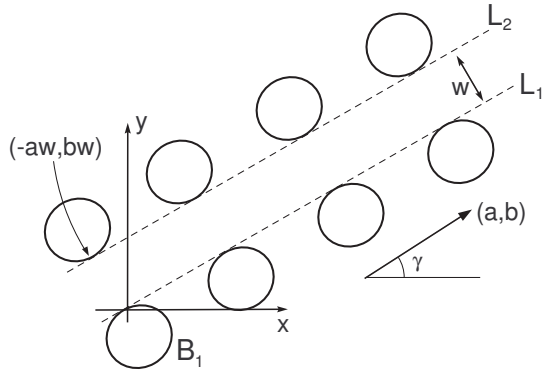


FIGURE 6. An infinite corridor bounded by two lines tangent to the scatterers.

First we note that the contribution from the lower cells $D_m^{(L)}$ is $\mathcal{O}(1)$, according to (10.2), hence they can be ignored. Second we can choose a large constant $M \gg 1$ and ignore all phase points with $\|\mathbf{\Delta}_\varepsilon\| \le M$. So we only consider trajectories that shoot from the initial scatterer facing an infinite corridor (see $B_1$ in Fig. 6) and landing on distant scatterers on the opposite side of that corridor (the upper row in Fig. 6).

Next, let $L_1$ and $L_2$ denote two parallel lines bordering our corridor, i.e. the two common tangent lines to all the scatterers along our corridor, see Fig. 6. Our trajectories leave the scatterer $B_1$, cross $L_1$ first, then after a long trip in the corridor they cross $L_2$ and land very shortly on the next scatterer in the top row. Let $\hat{\mathbf{\Delta}}_\varepsilon = (\hat{\mathbf{\Delta}}_{\varepsilon,x}, \hat{\mathbf{\Delta}}_{\varepsilon,y})$ denote the vector between the two crossing points, on $L_1$ and $L_2$ respectively. Note that $\Delta_{\varepsilon,x} = \hat{\mathbf{\Delta}}_{\varepsilon,x} + \mathcal{O}(1)$ and $\Delta_{\varepsilon,y} = \hat{\mathbf{\Delta}}_{\varepsilon,y} + \mathcal{O}(1)$, thus

$$\nu_0(\Delta_{\varepsilon,x}^2) = \nu_0(\hat{\mathbf{\Delta}}_{\varepsilon,x}^2) + \mathcal{O}(1), \qquad \nu_0(\Delta_{\varepsilon,x}\Delta_{\varepsilon,y}) = \nu_0(\hat{\mathbf{\Delta}}_{\varepsilon,x}\hat{\mathbf{\Delta}}_{\varepsilon,y}) + \mathcal{O}(1),$$

and so we can replace $\Delta_{\varepsilon,x}, \Delta_{\varepsilon,y}$ with $\hat{\mathbf{\Delta}}_{\varepsilon,x}, \hat{\mathbf{\Delta}}_{\varepsilon,y}$.

We again use the transformation $T$ that straightens all our trajectories and transforms the domain $\tilde{\mathcal{D}}$ into $\mathcal{Q} = T(\tilde{\mathcal{D}})$. The lines $L_1$ and

$L_2$ will be mapped into curves $T(L_1)$ and $T(L_2)$ in the $uv$ plane, see Fig. 7. Let us choose the coordinate system so that the line $L_1$ passes through the origin, and denote, as before, the width of the corridor by $w$ and the angle between the corridor and the field direction (i.e., the $x$ axis) by $\gamma$. Then the other line $L_2$ is given by parametric equations $x = as - bw$ and $y = bs + aw$, where $a = \cos\gamma$ and $b = \sin\gamma$ (note that $s$ is the arclength parameter on $L_1$). The curve $T(L_2)$ is now given by parametric equations

$$\begin{aligned} u &= \varepsilon^{-1}\big[e^{\varepsilon(as-bw)}\cos\varepsilon(bs+aw) - 1\big] \\ v &= \varepsilon^{-1}e^{\varepsilon(as-bw)}\sin\varepsilon(bs+aw). \end{aligned} \tag{10.3}$$

Recall that the expansion factor of the transformation $T$ is $e^{\varepsilon x} = 1 + \mathcal{O}(\sqrt{\varepsilon})$, hence we have $\hat{\mathbf{\Delta}}_{\varepsilon,x} = u + \mathcal{O}(1)$ and $\hat{\mathbf{\Delta}}_{\varepsilon,y} = v + \mathcal{O}(1)$, hence we can further replace $\hat{\mathbf{\Delta}}_{\varepsilon,x}, \hat{\mathbf{\Delta}}_{\varepsilon,y}$ with $u, v$. In the subsequent calculation $s$ will parameterize the intersections of our trajectories with $L_1$ and $L_2$.

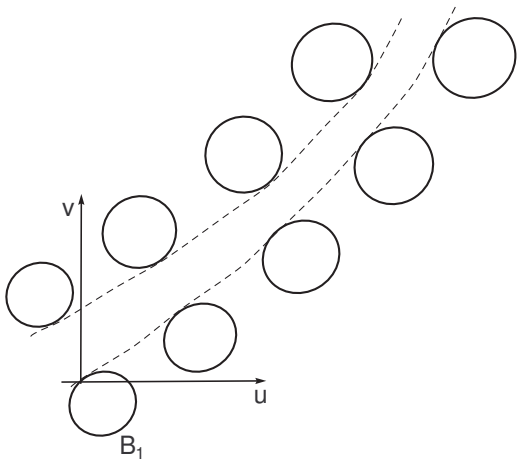


FIGURE 7. A transformed infinite corridor in the $uv$ plane bounded by two curves tangent to the scatterers.

Let $\theta$ denote the angle between the (straight) trajectory on the $uv$ plane and the horizontal $u$ axis. Let $D$ denote the distance between the consecutive scatterers tangent to the line $L_1$. Our trajectories then originate on the segment of length $D$ on the line $L_1$ and make an angle $\varphi = \theta - \gamma$ with it. Let us denote this segment by $\hat{L}_1$. We can regard it as an 'artificial' part of the boundary of our billiard table $\mathcal{Q}$, and then the image of the measure $\nu_0$ on it would be a smooth measure with density

$$c_\nu \cos\varphi \, dr \, d\varphi = c_\nu \sin(\theta - \gamma) \, dr \, d\theta,$$

where $r$ is the length parameter on $\hat{L}_1$ and $\varphi = \pi/2 - (\theta - \gamma)$ is the angle made by the outgoing trajectories with the normal to $\hat{L}_1$, cf. (1.1). Now the contribution of all the above trajectories to $\nu_0(\Delta_{\varepsilon,x}^2)$ will be

$$\mathcal{I} = c_\nu D \int_{s_{\min}}^{s_{\max}} u^2 \sin(\theta - \gamma)\, d\theta + \mathcal{O}(1) \tag{10.4}$$

for some $s_{\min} = \mathcal{O}(1)$ and $s_{\max} \sim C/\sqrt{\varepsilon}$. To deal with $\nu_0(\Delta_{\varepsilon,x}\Delta_{\varepsilon,y})$, we just replace $u^2$ with $uv$ in (10.4).

Now by elementary geometry

$$\sin(\theta - \gamma) = \frac{av - bu + \mathcal{O}(1)}{[u^2 + v^2]^{1/2}},$$

as well as

$$\begin{aligned} d\theta &= \frac{v\,\frac{du}{ds} - u\,\frac{dv}{ds} + \mathcal{O}(1)}{u^2 + v^2}\, ds \\ &= \left[\frac{av - bu + \mathcal{O}(1)}{u^2 + v^2} - \varepsilon b\right] ds. \end{aligned}$$

These formulas can be easily derived assuming that the starting point is $(0, 0)$, then the term $\mathcal{O}(1)$ is not needed; it only accounts for the variation of the starting point on the segment $\hat{L}_1$ of length $D = \mathcal{O}(1)$.

Now using Taylor expansion gives us the following: $u = as + \mathcal{O}(1)$, $v = bs + \mathcal{O}(1)$, $u^2 + v^2 = s^2 + \mathcal{O}(s)$, and

$$av - bu = w + \tfrac{1}{2}\, b\varepsilon s^2 + \mathcal{O}(\sqrt{\varepsilon}).$$

Substituting these formulas into (10.4) and integrating from 0 to $s_{\max} \sim C/\sqrt{\varepsilon}$ readily gives

$$\mathcal{I} = \tfrac{1}{2}\, c_\nu a^2 w^2 D |\ln \varepsilon| + \mathcal{O}(1),$$

and to deal with $\nu_0(\Delta_{\varepsilon,x}\Delta_{\varepsilon,y})$, we just replace $a^2$ with $ab$. It remains to sum up over all the infinite corridors and all the segments between consecutive scatterers on their borders. Then we obtain exactly

$$\begin{aligned} \nu_0(\Delta_{\varepsilon,x}^2) &= \hat{\mathbf{D}}_{x,x} |\ln \varepsilon| + \mathcal{O}(1) \\ \nu_0(\Delta_{\varepsilon,x}\Delta_{\varepsilon,y}) &= \hat{\mathbf{D}}_{x,y} |\ln \varepsilon| + \mathcal{O}(1), \end{aligned} \tag{10.5}$$

where $\hat{\mathbf{D}}_{\dots}$ denote the corresponding components of the superdiffusion matrix $\hat{\mathbf{D}}$ given by (2.1). This completes the proof of (4.6)–(4.8).

Next we prove (3.8)–(3.9) following our plan in Section 4. First we check that the convergence of the series (4.9), with the exception of the term $n = 0$, is exponential and uniform in $\varepsilon$. This follows from (9.13) in Proposition 9.3. Second, we already established that $\nu_\varepsilon(\boldsymbol{\Delta}_\varepsilon) = \mathcal{O}(1)$; see e.g. (9.17).

It remains to bounds the series

$$\sum_{k=1}^{\infty} \nu_0\big[(\Delta_{\varepsilon,x}^2 \circ \mathcal{F}_\varepsilon^k)(1-g)\big] = \varepsilon \sum_{n=1}^{\infty} \nu_0\big[(\Delta_{\varepsilon,x}^2 \circ \mathcal{F}_\varepsilon^n)(\Delta_{\varepsilon,x} + \mathcal{R}_\varepsilon)\big]$$

that appears in (4.11). We will apply the same argument as in (9.15)–(9.16). First, due to (8.3) we have

$$\sum_{k=n}^{\infty} \nu_0\big[(\Delta_{\varepsilon,x}^2 \circ \mathcal{F}_\varepsilon^k)(1-g)\big] \le C\varepsilon^{-1}\theta^n$$

for all $n \ge 1$, with a constant $\theta < 1$. Setting $n = L|\log\varepsilon|$ with a sufficiently large $L > 0$ gives a tail bound $\mathcal{O}(1)$, so it remains to deal with $n < L|\log\varepsilon|$. To this end we use Hölder inequality

$$\big|\nu_0\big[(\Delta_{\varepsilon,x}^2 \circ \mathcal{F}_\varepsilon^n)(\Delta_{\varepsilon,x} + \mathcal{R}_\varepsilon)\big]\big| \le \big[(\nu_0 \circ \mathcal{F}_\varepsilon^n)\big(|\Delta_{\varepsilon,x}^3|\big)\big]^{2/3} \big[\nu_0\big(|\Delta_{\varepsilon,x} + \mathcal{R}_\varepsilon|^3\big)\big]^{1/3},$$

and each of these integrals is bounded by

$$C\sum_{m=1}^{m_U} \frac{m^3}{m^3} + C\sum_{m=1}^{m_L} \frac{m^4}{m_L^4} \le C(m_U + m_L) \le C/\sqrt{\varepsilon},$$

recall Lemma 8.1 and the proof of Proposition 8.3. Summing over $n \le L|\log\varepsilon|$ gives

$$\varepsilon \sum_{n=1}^{L|\log\varepsilon|} \nu_0\big[(\Delta_{\varepsilon,x}^2 \circ \mathcal{F}_\varepsilon^n)(\Delta_{\varepsilon,x} + \mathcal{R}_\varepsilon)\big] \le C\sqrt{\varepsilon}\,|\log\varepsilon|,$$

which completes the proof of Theorem 9.

We turn to the proof of Proposition 3.1 following our plan in the end of Section 4. First, one can check directly that the collision time function $\tau_\varepsilon$ has all the same properties as the displacement function $\Delta_\varepsilon$, hence the series (4.12) converges exponentially and uniformly in $\varepsilon$. So it is enough to prove (4.13), and this requires geometric analysis.

It is easy to see by (5.1) that if a trajectory starts from a phase point $(\mathbf{q}, \mathbf{v})$ and moves without collisions for a time $\tau$, then it deviates from a billiard trajectory starting from the same phase point by $\mathcal{O}(\varepsilon\tau^2)$. Thus, on most part of the space $\mathcal{M}$ we have $|\tau_\varepsilon - \tau| = \mathcal{O}(\varepsilon)$. The only exceptions will be (i) the $\mathcal{O}(\varepsilon)$-neighborhood of singularity lines (where the images of points under $\mathcal{F}$ and $\mathcal{F}_\varepsilon$ may land on different scatterers so that $|\tau_\varepsilon - \tau| = \mathcal{O}(1)$) and (ii) the cells $D_m$, $D_m^{(U)}$, and $D_m^{(L)}$ (which were described earlier), on which either $\tau$ or $\tau_\varepsilon$, respectively, is large.

Let $b > 0$ be a small constant. The contribution to (4.13) from all the cells $D_m$, $D_m^{(U)}$ with $m \geq \varepsilon^{-b}$ will be bounded by

$$C \sum_{m=\varepsilon^{-b}}^{\infty} \frac{m}{m^3} = C\varepsilon^b,$$

because $\tau \sim Cm$ on $D_m$ and $\tau_\varepsilon \sim Cm$ on $D_m^{(U)}$; thus all such cells can be discarded. The 'lower' cells $D_m^{(L)}$ can be discarded altogether, as

$$\sum_{m=1}^{m_L} \frac{m^2}{m_L^4} = \mathcal{O}(m_L^{-1}) = \mathcal{O}(\varepsilon^{1/2}).$$

Let $X \in D_m^{(U)}$. If the images of $X$ under the maps $\mathcal{F}_\varepsilon$ and $\mathcal{F}$ land on the same scatterer, then they will be $\mathcal{O}(m\sqrt{\varepsilon})$ apart, because their trajectories will run $\mathcal{O}(m^2\varepsilon)$-close. Hence such points make a total contribution of

$$C \sum_{m=1}^{\varepsilon^{-b}} \frac{m\sqrt{\varepsilon}}{m^3} \leq C\sqrt{\varepsilon}.$$

If the images of $X \in D_m^{(U)}$ under the maps $\mathcal{F}_\varepsilon$ and $\mathcal{F}$ land on different scatterers, then one of them lands in the $\mathcal{O}(m\sqrt{\varepsilon})$-vicinity of the edge of $\mathcal{M}$ (defined by $\varphi = \pm\pi/2$), and thus $X$ must be in the $\mathcal{O}(\sqrt{\varepsilon})$-vicinity of the boundary of the cell $D_m^{(U)}$ (as the expansion factor is at least $\geq Cm$). For $m < \varepsilon^{-b}$, the width of the cells $D_m^{(U)}$ and $D_m$ is $\sim Cm^{-2} \gg \sqrt{\varepsilon}$, thus $X$ belongs to $D_{m'}$ with $m' = m \pm 1$, i.e. $|\tau_\varepsilon - \tau_0| = \mathcal{O}(1)$. Thus the contribution of all such points is

$$C \sum_{m=1}^{\varepsilon^{-b}} \frac{\sqrt{\varepsilon}}{m} \leq C\sqrt{\varepsilon}\,|\ln\varepsilon|.$$

Combining all our estimates proves (4.13), and hence we complete the proof of Proposition 3.1. □

## 11. Proof of Theorem 8

Here we prove the discrete-time Theorem 8 on superdiffusion in field-free Lorentz gases, modulo some technical moment estimates to be completed in the next section. We begin with part (a) and then describe the modifications needed for part (b).

Recall that

$$\tilde{\mathbf{q}}_n - \tilde{\mathbf{q}}_0 = \boldsymbol{\Delta}_0 + \boldsymbol{\Delta}_1 + \cdots + \boldsymbol{\Delta}_{n-1}$$

where $\mathbf{\Delta}_j = \tilde{\mathbf{q}}_{j+1} - \tilde{\mathbf{q}}_j$ denotes the displacement vector between successive collisions. First we cut off the unbounded function $\mathbf{\Delta}$ as follows:

$$\hat{\mathbf{\Delta}}_j = \mathbf{\Delta}_j \mathbf{1}_{\|\mathbf{\Delta}_j\|<R}, \qquad R = \sqrt{n}/\ln^{100} n. \tag{11.1}$$

**Lemma 11.1.** *We have the following convergence in probability:*

$$\max_{m\le n} \frac{\tilde{\mathbf{q}}_m - \sum_{j=0}^{m-1} \hat{\mathbf{\Delta}}_j}{\sqrt{n\log n}} \to 0.$$

All the lemmas will be proved in the next section. We continue the proof of Theorem 8. Lemma 11.1 allows us to replace the unbounded function $\mathbf{\Delta}$ with its trimmed version $\hat{\mathbf{\Delta}}$.

Next we shall use standard Bernstein's method based on the 'big small block' technique. That is, we divide the time interval $[1, n]$ into big blocks of length $N \sim n^{0.6}$ alternating with small blocks of length $\sim n^{0.01}$ (starting with a small block). Accordingly let

$$\mathbf{Q}_k = \sum_{j=(n^{0.01}+N)(k-1)}^{n^{0.01}k+N(k-1)-1} \hat{\mathbf{\Delta}}_j,$$

$$\mathbf{Z}_k = \sum_{n^{0.01}k+N(k-1)}^{j=(n^{0.01}+N)k-1} \hat{\mathbf{\Delta}}_j.$$

Thus $\mathbf{Z}_k$ are sums over the big blocks and $\mathbf{Q}_k$ are the sums over the small blocks.

**Lemma 11.2.** *We have the following convergence in probability:*

$$\frac{\sum_k \mathbf{Q}_k}{\sqrt{n\log n}} \to 0.$$

Thus it is enough to analyze the big blocks only. They are separated by gaps (made by small blocks), which make the sums $\mathbf{Z}_k$ in different big blocks nearly independent. To make this statement precise, let

$$m'_k = (n^{0.01} + N)k + \tfrac{1}{3}\, n^{0.01}$$

be a moment within a small block, $\frac{1}{3}\, n^{0.01}$ collisions away from the previous big block. The measure $\nu_0$ can be represented as $\mathbb{P}_{\mathcal{G}_0}$ for a proper standard family; see the end of Section 6. The preimages of curves $W \in \mathcal{G}_0$ are exponentially small at time $(n^{0.01} + N)k$, i.e. at the end of the previous big block; hence the function $\hat{\mathbf{\Delta}}$ measured at times $j \le (n^{0.01} + N)k$ can be replaced with a constant, up to an exponentially small (more precisely, $\mathcal{O}\big(\theta^{n^{0.01}} R\big)$) error, on such curves. Now, at the time

$$m''_k = (n^{0.01} + N)k + \tfrac{2}{3}\, n^{0.01}$$

all the curves $W \in \mathcal{G}_0$ of length $\geq \theta^{\frac{1}{3}n^{0.01}}$ will grow to proper families (the curves of length $< \theta^{\frac{1}{3}n^{0.01}}$ make a set of exponentially small measure). Then we will take averages of the function $\hat{\mathbf{\Delta}}$ measured at times $j \geq (n^{0.01} + N)k + n^{0.01}$, corresponding to the next big block, with respect to measures $\mathbb{P}_{\mathcal{G}}$ on proper families at time $m''_k$. Those averages are expressed by formulas independent of $\mathcal{G}$ (see Lemma 11.3), hence the dynamics on different big blocks are practically independent.

**Lemma 11.3.** *Let* $\mathbf{Z}$ *denote a shifted big block*

$$\mathbf{Z} = \sum_{j=\frac{1}{3}n^{0.01}}^{\frac{1}{3}n^{0.01}+N} \hat{\mathbf{\Delta}}_j. \tag{11.2}$$

*Then for any proper standard family* $\mathcal{G}$ *at time zero*

$$\mathbb{P}_{\mathcal{G}}(\mathbf{Z}) = \mathcal{O}(\theta^{\frac{1}{4}n^{0.01}}) \tag{11.3}$$

$$\mathbb{P}_{\mathcal{G}}(\mathbf{Z} \otimes \mathbf{Z}) = 2N\hat{\mathbf{D}} \ln R + \mathcal{O}(N) \tag{11.4}$$

$$\mathbb{P}_{\mathcal{G}}\big(\|\mathbf{Z}\|^4\big) = \mathcal{O}\big(NR^2 \ln^3 n + N^2 \ln^2 n\big). \tag{11.5}$$

*Here* $\hat{\mathbf{D}}$ *is the discrete-time superdiffusion matrix given by* (2.1).

Next we derive Theorem 8(a) from this lemma by using characteristic functions. Let

$$\phi_m(\xi) = \nu_0\left(\exp\left(\sum_{k=1}^{m} \frac{i\langle \xi, \mathbf{Z}_k\rangle}{\sqrt{n \ln n}}\right)\right).$$

According to our discussion before Lemma 11.3, the dynamics within different big blocks is nearly independent in the sense that

$$\phi_m(\xi) = \prod_{k=1}^{m} \mathbb{P}_{\mathcal{G}_k}\left(\exp\left(\frac{i\langle \xi, \mathbf{Z}_k\rangle}{\sqrt{n \ln n}}\right)\right) + \mathcal{O}\big(\theta_1^{n^{0.01}}\big),$$

for some $\theta_1 < 1$ and some proper standard families $\mathcal{G}_k$, each taken at the time $m''_{k-1}$, i.e. $\frac{1}{3}n^{0.01}$ collisions prior to the big block $\mathbf{Z}_k$. Now we use Taylor expansion

$$\exp\left(\frac{i\langle \xi, \mathbf{Z}_k\rangle}{\sqrt{n \ln n}}\right) = 1 + \frac{i\langle \xi, \mathbf{Z}_k\rangle}{\sqrt{n \ln n}} - \frac{\langle \xi, \mathbf{Z}_k\rangle^2}{2n \ln n} + \mathcal{O}\left(\frac{\|\mathbf{Z}_k\|^3}{(n \ln n)^{3/2}}\right)$$

and by Lemma 11.3 the $\mathbb{P}_{\mathcal{G}_k}$-average of the first three terms is

$$1 - \frac{2\langle \hat{\mathbf{D}}\xi, \xi\rangle N \ln R}{2n \ln n} + o\Big(\frac{N}{n}\Big) = 1 - \frac{\langle \hat{\mathbf{D}}\xi, \xi\rangle N}{2n} + o\Big(\frac{N}{n}\Big).$$

The average of the last term is estimated by the Cauchy-Schwartz inequality:

$$\begin{aligned}\mathbb{P}_{\mathcal{G}_k}(\|\mathbf{Z}_k\|^3) &\le \left[\mathbb{P}_{\mathcal{G}_k}(\|\mathbf{Z}_k\|^2)\,\mathbb{P}_{\mathcal{G}_k}(\|\mathbf{Z}_k\|^4)\right]^{1/2}\\ &= \mathcal{O}\left(NR\ln^2 n + (N\ln n)^{3/2}\right)\end{aligned}$$

so its contribution will be negligible. Note that our estimates are independent of the standard family $\mathbb{P}_{\mathcal{G}_k}$. Hence we obtain

$$\ln \phi_m(\xi) = -\frac{m\langle \hat{\mathbf{D}}\xi,\xi\rangle N}{2n} + o\Big(\frac{mN}{n}\Big)$$

and taking $m = n/(N+n^{0.01})$ we get

$$\nu_0\left(\exp\left(\frac{i\langle \xi, \tilde{\mathbf{q}}_n\rangle}{\sqrt{n\ln n}}\right)\right) \to \exp\left(-\frac{\langle \hat{\mathbf{D}}\xi,\xi\rangle}{2}\right)$$

as $n\to\infty$. This implies the weak convergence to a normal distribution claimed in Theorem 4. Our proof is different from the one given in [28]; the latter uses spectral properties of the corresponding transfer operator.

To prove the weak convergence to a Brownian motion claimed in Theorem 8(a) we need two more properties: (i) the weak convergence of finite-dimensional distributions of $\frac{\mathbf{q}_{sn}}{\sqrt{n\ln n}}$ to those of the Brownian Motion, and (ii) the tightness, see below. To derive (i) let

$$\frac{n_1}{n}\to s_1, \frac{n_2}{n}\to s_2, \dots, \frac{n_k}{n}\to s_k,$$

then the same argument as above shows that for any $\xi_1,\xi_2,\dots,\xi_k$

$$\nu_0\left(\exp\left(\frac{i\sum_{j=1}^k\langle \xi_j, \tilde{\mathbf{q}}_{n_j}\rangle}{\sqrt{n\ln n}}\right)\right) \to \prod_{j=1}^k \exp\left(-\frac{\langle \hat{\mathbf{D}}\eta_j,\eta_j\rangle (s_j-s_{j-1})^2}{2}\right)$$

where $s_0=0$ and $\eta_j=\sum_{p=1}^j \xi_p$. This convergence implies (i).

It remains to show that the family of functions

$$\{W_n(s)\} = \{S_{ns}/\sqrt{n\ln n}\}, \qquad 0<s<1$$

is tight, where $S_n=\sum_{j\le n}\hat{\mathbf{\Delta}}_j$. By the standard argument (see e.g. [1], Chapter 2) it is enough to show that there exists a sequence $\{\delta_k\}$ with $\sum_k \delta_k<\infty$ such that $\nu_0(\mathcal{M}_{K,n})\to 0$ as $K\to\infty$ uniformly in $n$, where

$$\mathcal{M}_{K,n} = \left\{\exists j,k\colon \tfrac{j}{2^k}<1 \text{ and } \left|W_n\left(\tfrac{j+1}{2^k}\right) - W_n\left(\tfrac{j}{2^k}\right)\right| > K\delta_k\right\}. \tag{11.6}$$

Let $\delta_k = 1/k^2$. We need to estimate the probability that

$$|S_{n_2}-S_{n_1}| \ge \frac{K\sqrt{n\ln n}}{k^2} \tag{11.7}$$

where $n_2 - n_1 \sim n/2^k$. Observe that $|S_{n_2} - S_{n_1}| \le Rn/2^k$, hence (11.7) is impossible if $k^2/2^k < 1/n$, in particular if $k > C \ln n$, where $C \gg 1$ is a large constant. For $k < C \ln n$, we use Lemma 11.3(c) and the Markov inequality to estimate the probability of (11.7) by

$$\frac{k^8 \nu_0\big([S_{n_2} - S_{n_1}]^4\big)}{K^4 n^2 \ln^2 n} \le Ck^8 \frac{(n_2 - n_1) R^2 \ln^3 n + (n_2 - n_1)^2 \ln^2 n}{K^4 n^2 \ln^2 n}$$
$$= \frac{Ck^8}{K^4} \left( \frac{1}{2^k \ln^{99} n} + \frac{1}{4^k} \right).$$

Since (11.6) includes $2^k$ intervals of size $2^{-k}$ we get

$$\nu_0(\mathcal{M}_{K,n,k}) \le \frac{Ck^8}{K^4} \left( \frac{1}{\ln^{99} n} + \frac{1}{2^k} \right).$$

where $\mathcal{M}(K, n, k)$ denotes the part of the set (11.6) corresponding to a particular $k$. Summing over $k \le C \ln n$ we see that $\nu_0(\mathcal{M}_{K,n}) \le C/K \to 0$, as $K \to \infty$, uniformly in $n$, which implies the tightness. This completes the proof of Theorem 8(a).

The proof of part (b) proceeds along the same lines as the proof of part (a), with some modifications that we describe next. First, only the $x$-component of the displacement vector $\boldsymbol{\Delta} = (\Delta_x, \Delta_y)$ is unbounded, its $y$-component is bounded and quite regular (dynamically Hölder continuous). Thus we redefine $\hat{\boldsymbol{\Delta}}_j$ in (11.1) as follows:

$$\hat{\boldsymbol{\Delta}}_j = \big(\Delta_{j,x} \mathbf{1}_{|\Delta_{j,x}| < R},\ \Delta_{j,y}\big), \tag{11.8}$$

i.e. we only trim the $x$-components. Now the components of the vector $\mathbf{Z} = (\mathbf{Z}_x, \mathbf{Z}_y)$ in Lemma 11.3 will play different roles, and the lemma is modifies as follows (see the proof in the next section):

**Lemma 11.4.** *Under the assumptions of Theorem 8(b), and in the notation of Lemma 11.3*

$$\begin{aligned}
\mathbb{P}_{\mathcal{G}}(\mathbf{Z}) &= \mathcal{O}\big(\theta^{\frac{1}{4} n^{0.01}}\big) \\
\mathbb{P}_{\mathcal{G}}(\mathbf{Z}_x^2) &= 2N \hat{\mathbf{D}}_{xx} \ln R + \mathcal{O}(N) \\
\mathbb{P}_{\mathcal{G}}(\mathbf{Z}_y^2) &= N \hat{\mathbf{D}}^*_{yy} + \mathcal{O}(1) \\
\mathbb{P}_{\mathcal{G}}(\mathbf{Z}_x \mathbf{Z}_y) &= \mathcal{O}(N) \\
\mathbb{P}_{\mathcal{G}}\big(\mathbf{Z}_x^4\big) &= \mathcal{O}\big(NR^2 \ln^3 n + N^2 \ln^2 n\big). \\
\mathbb{P}_{\mathcal{G}}\big(\mathbf{Z}_y^4\big) &= \mathcal{O}(N^2).
\end{aligned}$$

Then the proof Theorem 8(b) proceeds as the proof of part (a). □

## 12. Moment Estimates

Here we prove the four lemmas from the previous section by using standard moment estimates. First, due to (9.11)–(9.12) and Corollary 9.2 we have

$$\nu_0(\hat{\mathbf{\Delta}}_j) = 0, \qquad \nu_0(\hat{\mathbf{\Delta}}_j \otimes \hat{\mathbf{\Delta}}_j) = \mathcal{O}(\ln R), \tag{12.1}$$

and, for $i \neq j$

$$\nu_0(\hat{\mathbf{\Delta}}_i \otimes \hat{\mathbf{\Delta}}_j) = \mathcal{O}\big(\theta^{|i-j|}\big). \tag{12.2}$$

Moreover, the second formula in (12.1) can be specified as follows:

$$\nu_0(\hat{\mathbf{\Delta}}_j \otimes \hat{\mathbf{\Delta}}_j) = 2\hat{\mathbf{D}} \ln R + \mathcal{O}(1), \tag{12.3}$$

where $\hat{\mathbf{D}}$ is the discrete-time superdiffusion matrix given by (2.1). The proof of (12.3) goes by direct integration similar to our calculations in Section 10; in fact the present case is much simpler because the structure of the scatterers is periodic; we leave the details to the reader (the formula (12.3) is effectively obtained in [28], but without an explicit proof).

*Proof of Lemma 11.2.* We estimate the second moment. Let $\mathbf{Q} = \sum_k \mathbf{Q}_k$. Note that the total number of terms in the small blocks is $n^{1.01}/N$. Due to (12.3)–(12.2) we have

$$\nu_0(\mathbf{Q} \otimes \mathbf{Q}) = \mathcal{O}\big[(\ln R)\, n^{1.01}/N + R^{-2} n^{2.02}/N^2 + n^{1.01}/N\big],$$

the last term comes from the convergent series $\sum_m \theta^m$. Thus

$$\frac{\nu_0(\mathbf{Q} \otimes \mathbf{Q})}{n \log n} \to 0 \quad \text{as} \quad n \to \infty,$$

and Lemma 11.2 follows from Chebychev's inequality. □

Next, the function $\hat{\mathbf{\Delta}}$ defined by (11.1) is dynamically Hölder continuous with parameters $\theta_{\hat{\mathbf{\Delta}}} < 1$ (independent of the cut-off value $R$) and $K_{\hat{\mathbf{\Delta}}} = \mathcal{O}(R)$; we also have $\|\hat{\mathbf{\Delta}}\|_\infty = \mathcal{O}(R)$. Thus, due to Theorem 10, for any proper standard family $\mathcal{G}$ and $i \geq 0$

$$\mathbb{P}_{\mathcal{G}}(\hat{\mathbf{\Delta}}_i) = \nu_0(\hat{\mathbf{\Delta}}_i) + \mathcal{O}(\theta^i R) = \mathcal{O}(\theta^i R) \tag{12.4}$$

for some constant $\theta < 1$. Similarly, the multiple-time version of Theorem 10 (see, e.g. [13, Theorem 7.33]) implies that for any $p \geq 1$ and $i_1 \leq i_2 \leq \cdots \leq i_p$ we have

$$\mathbb{P}_{\mathcal{G}}(\hat{\mathbf{\Delta}}_{i_1} \otimes \cdots \otimes \hat{\mathbf{\Delta}}_{i_p}) = \nu_0(\hat{\mathbf{\Delta}}_{i_1} \otimes \cdots \otimes \hat{\mathbf{\Delta}}_{i_p}) + \mathcal{O}(\theta^{i_1} R^p). \tag{12.5}$$

We will only need this estimate for $p = 2$ and $p = 4$.

*Proof of Lemma 11.3.* The first moment estimate (11.3) follows from (12.4):

$$\mathbb{P}_{\mathcal{G}}(\mathbf{Z}) = \mathcal{O}\big(\theta^{\frac{1}{3}n^{0.01}} R\big) = \mathcal{O}\big(\theta^{\frac{1}{4}n^{0.01}}\big)$$

The second moment estimate (11.4) follows from (12.2)–(12.5):

$$\begin{aligned}\mathbb{P}_{\mathcal{G}}(\mathbf{Z}\otimes\mathbf{Z}) &= \sum_{i,j} \mathbb{P}_{\mathcal{G}}(\hat{\mathbf{\Delta}}_i \otimes \hat{\mathbf{\Delta}}_j) \\ &= \sum_{i,j} \nu_0(\hat{\mathbf{\Delta}}_i \otimes \hat{\mathbf{\Delta}}_j) + \mathcal{O}\big(N^2 R^2 \theta^{\frac{1}{3}n^{0.01}}\big) \\ &\sim 2N\hat{\mathbf{D}} \ln R + \mathcal{O}(N).\end{aligned}$$

where the summation runs over $i, j$ given by (11.2).

To prove the fourth moment estimate (11.5) we put $\hat{\mathbf{\Delta}}_j = (\hat{\Delta}_{j,x}, \hat{\Delta}_{j,y})$; then by Cauchy-Schwarz inequality

$$\|\mathbf{Z}\|^4 \le 2\Big(\sum_j \hat{\Delta}_{j,x}\Big)^4 + 2\Big(\sum_j \hat{\Delta}_{j,y}\Big)^4,$$

where the summation runs over $j$ specified by (11.2). Since both $\hat{\Delta}_{j,x}$ and $\hat{\Delta}_{j,y}$ will be treated similarly, we will drop the indices $x$ and $y$. Expanding the fourth powers we get the sums of various products

$$\hat{\Delta}_{j_1}\hat{\Delta}_{j_2}\hat{\Delta}_{j_3}\hat{\Delta}_{j_4}, \qquad j_1 \le j_2 \le j_3 \le j_4. \tag{12.6}$$

Due to (12.5) we have

$$\mathbb{P}_{\mathcal{G}}\big(\hat{\Delta}_{j_1}\hat{\Delta}_{j_2}\hat{\Delta}_{j_3}\hat{\Delta}_{j_4}\big) = \nu_0\big(\hat{\Delta}_{j_1}\hat{\Delta}_{j_2}\hat{\Delta}_{j_3}\hat{\Delta}_{j_4}\big) + \mathcal{O}(\theta^{\frac{1}{3}n^{0.01}} R^4)$$

We fix a large constant $C_1 \gg 1$ and divide the products (12.6) into three categories depending on the gaps between indices

$$D_1 = j_2 - j_1, \quad D_2 = j_3 - j_2, \quad D_3 = j_4 - j_3.$$

**Case 1** (most significant): $|D_i| \le C_1 \ln n$ for all $i = 1, 2, 3$. Then by Hölder inequality

$$\big|\nu_0\big(\hat{\Delta}_{j_1}\hat{\Delta}_{j_2}\hat{\Delta}_{j_3}\hat{\Delta}_{j_4}\big)\big| \le \nu_0(\hat{\Delta}^4) \le C\sum_{m=1}^{R} \frac{m^4}{m^3} \le CR^2,$$

thus the total contribution of such terms is $\mathcal{O}\big(NR^2 \ln^3 n\big)$.

**Case 2** (of moderate significance): $|D_2| > C_1 \ln n$ and $|D_i| \le C_1 \ln n$ for $i = 1, 3$. Then by standard correlation estimates [13, Section 7.7] and again Hölder inequality we have

$$\begin{aligned}\nu_0\big(\hat{\Delta}_{j_1}\hat{\Delta}_{j_2}\hat{\Delta}_{j_3}\hat{\Delta}_{j_4}\big) &= \big[\nu_0\big(\hat{\Delta}^2\big)\big]^2 + \mathcal{O}(R^4\theta^{C_1 \ln n}) \\ &= \mathcal{O}\big(\ln^2 R\big) + \mathcal{O}\big(n^{-100}\big).\end{aligned}$$

Thus the total contribution of such terms is $\mathcal{O}\big(N^2 \ln^2 n\big)$.

**Case 3**: (least significant): $|D_1| > C_1 \ln n$ or $|D_3| > C_1 \ln n$. In this case, since $\nu_0(\hat{\Delta}) = 0$, the correlation estimates will easily give an upper bound of $\mathcal{O}\big(n^{-100}\big)$.

Lemma 11.3 is proven. □

*Proof of Lemma 11.1.* The reason why $\tilde{\mathbf{q}}_n \neq \sum_{j=0}^{n-1} \hat{\mathbf{\Delta}}_j$ is that some $\mathbf{\Delta}_j$ take large values exceeding $R$. We split our argument into two parts. First we set

$$R' = \sqrt{n} \ln \ln n$$

and show that values of $\mathbf{\Delta}_j$ exceeding $R'$ can be disregarded since their probabilities are negligibly small. Indeed, due to (3.1)

$$\nu_0\big(\exists j \le n \colon \|\mathbf{\Delta}_j\| > R'\big) = \mathcal{O}\big((\ln \ln n)^{-2}\big) \to 0.$$

Next we show that moderately large values of $\mathbf{\Delta}_j$ (those between $R$ and $R'$), albeit rather frequent, tend to cancel each other. Let

$$\tilde{\mathbf{\Delta}}_j = \mathbf{\Delta}_j \mathbf{1}_{R \le \|\mathbf{\Delta}_j\| \le R'}, \qquad \tilde{S}_m = \sum_{j=0}^{m-1} \tilde{\mathbf{\Delta}}_j.$$

Note that

$$\nu_0(\tilde{\mathbf{\Delta}}_j) = 0, \qquad \nu_0(\tilde{\mathbf{\Delta}}_j \otimes \tilde{\mathbf{\Delta}}_j) \le C \sum_{m=R}^{R'} \frac{m^2}{m^3} \le C \ln \ln n.$$

Arguing as in the proof of the second moment estimate in Lemma 11.3 we get, for every $m \le n$

$$\nu_0\big(\tilde{S}_m \otimes \tilde{S}_m\big) \le Cm \ln \ln n,$$

and so by Chebyshev inequality for any $\epsilon > 0$

$$\nu_0\big(\|\tilde{S}_m\| \ge \epsilon \sqrt{n \ln n}\big) \to 0, \tag{12.7}$$

uniformly in $m$. But need to obtain a stronger estimate:

$$\nu_0\Big(\max_{1 \le m \le n} \|\tilde{S}_m\| \ge \epsilon \sqrt{n \ln n}\Big) \to 0. \tag{12.8}$$

To this end we will show that the sets

$$\mathcal{M}_{m,\epsilon} = \{X \in \mathcal{M} \colon \|\tilde{S}_m\| \ge \epsilon \sqrt{n \ln n}\}.$$

tend to overlap heavily. First note that

$$\nu_0\big(\mathcal{M}_{m,\epsilon} \setminus \mathcal{M}_{m-1,\epsilon}\big) \le \nu_0(\tilde{\mathbf{\Delta}}_{m-1} \neq 0) \le \frac{C \ln^{200} n}{n}.$$

where the last bound follows from (3.1). Next we show that

$$\nu_0\big((\mathcal{M}_{m,\epsilon} \setminus \mathcal{M}_{m-1,\epsilon}) \setminus \mathcal{M}_{n,\epsilon/2}\big) \le \delta_n \nu_0\big(\mathcal{M}_{m,\epsilon} \setminus \mathcal{M}_{m-1,\epsilon}\big) \tag{12.9}$$

where $\delta_n \to 0$ as $n \to \infty$. Then a simple summation over $m = 1, \dots, n$ will imply

$$\nu_0\left(\bigcup_{m=1}^{n} \mathcal{M}_{m,\epsilon}\right) \le \delta_n + \nu_0\left(\mathcal{M}_{n,\epsilon/2}\right).$$

Combining this with (12.7) we will obtain (12.8).

Our proof of (12.9) resembles the reflection principle in the theory of random walks. We note that each point of the set on the left hand side of (12.9) satisfies (simultaneously) three conditions:

$$\tilde{\mathbf{\Delta}}_{m-1} \neq 0, \quad \Big\|\sum_{j=0}^{m-1} \tilde{\mathbf{\Delta}}_j\Big\| \ge \epsilon\sqrt{n \ln n}, \quad \Big\|\sum_{j=m}^{n-1} \tilde{\mathbf{\Delta}}_j\Big\| \ge \tfrac{1}{2}\,\epsilon\sqrt{n \ln n}.$$

Since $\tilde{\mathbf{\Delta}}_{m-1} \neq 0$, we have $\|\mathbf{\Delta}_{m-1}\| \ge R = \sqrt{n}/\ln^{100} n$. A standard property of the Lorentz gas is that whenever $\mathbf{\Delta}_{m-1}$ is large, then typically $\|\mathbf{\Delta}_m\| \sim \|\mathbf{\Delta}_{m-1}\|^{1/2}$, then $\|\mathbf{\Delta}_{m+1}\| \sim \|\mathbf{\Delta}_{m-1}\|^{1/4}$, etc. Precisely, there exist $p, q > 0$ such that for any large $C_2 > 0$ there exists $C_3 > 0$ such that

$$\begin{aligned}\nu_0\Big(\|\mathbf{\Delta}_{m-1}\| \ge R \ \text{ and } \max_{0\le k\le C_2 \ln n} \|\mathbf{\Delta}_{m+k}\| > \|\mathbf{\Delta}_{m-1}\|^{1-q}\Big)& \\ \le C_3 R^{-p} \nu_0\big(\|\mathbf{\Delta}_{m-1}\| \ge R\big) \le C_3 R^{-(2+p)},&\end{aligned}$$

see [15, Lemma 5.1], and this measure is clearly negligibly small. Thus we can assume that whenever $\tilde{\mathbf{\Delta}}_{m-1} \neq 0$, we have $\tilde{\mathbf{\Delta}}_{m+k} = 0$ for all $k = 0, 1, \dots, C_2 \ln n$.

For $k > C_2 \ln n$, the correlations between $\tilde{\mathbf{\Delta}}_j$, $j \le m$, and $\tilde{\mathbf{\Delta}}_{m+k}$ are small, say they are $< n^{-200}$ if $C_2$ is large enough. Thus we have

$$\begin{aligned}\nu_0\big((\mathcal{M}_{m,\epsilon} \setminus \mathcal{M}_{m-1,\epsilon}) \setminus \mathcal{M}_{n,\epsilon/2}\big) &= \nu_0\big(\mathcal{M}_{m,\epsilon} \setminus \mathcal{M}_{m-1,\epsilon}\big) \\ &\times \nu_0\Big(\Big\|\sum_{j=m+C_2 \ln n}^{n-1} \tilde{\mathbf{\Delta}}_j\Big\| \ge \tfrac{1}{2}\,\epsilon\sqrt{n \ln n}\Big) + \mathcal{O}\big(n^{-100}\big),\end{aligned}$$

and the second factor on the right hand side converges to zero uniformly in $m$ due to (12.7). This completes the proof of (12.9). Thus (12.8) is proved, which implies Lemma 11.1. □

*Proof of Lemma 11.4.* The estimates dealing with $\mathbf{Z}_x$ alone are derived in the same way as in Lemma 11.3. Those dealing with $\mathbf{Z}_y$ alone are

quite standard (see e.g. [4] or [17, Section 9] or [13, Chapter 7]), because $\Delta_y$ is bounded and dynamically Hölder continuous. It remains to estimate the cross product term

$$\mathbb{P}_{\mathcal{G}}(\mathbf{Z}_x\mathbf{Z}_y) = \sum_{i,j} \mathbb{P}_{\mathcal{G}}(\hat{\Delta}_{i,x}\Delta_{j,y}).$$

As before, we trim the large component $\hat{\Delta}_{i,x}$ as

$$\hat{\Delta}_{i,x} = \hat{\Delta}'_{i,x} + \hat{\Delta}''_{i,x}, \qquad \hat{\Delta}'_{i,x} = \hat{\Delta}_{i,x}\mathbf{1}_{|\hat{\Delta}_{i,x}|<H}$$

where the cut-off value $H = H_{ij}$ will be chosen below. Then again

$$\mathbb{P}_{\mathcal{G}}(\hat{\Delta}'_{i,x}\Delta_{j,y}) = \mathcal{O}\big(H\theta_1^{|i-j|}\big)$$

for some $\theta_1 < 1$, whereas by (12.4) and the boundedness of $\Delta_{j,y}$

$$\begin{aligned}\big|\mathbb{P}_{\mathcal{G}}(\hat{\Delta}''_{i,x}\Delta_{j,y})\big| &\le C\mathbb{P}_{\mathcal{G}}(|\hat{\Delta}''_{i,x}|)\\ &\le C\nu_0(|\hat{\Delta}''_{i,x}|) + C\theta^{\frac13 n^{0.01}}R\\ &\le CH^{-1} + C\theta^{\frac14 n^{0.01}}.\end{aligned}$$

Choosing $H = \theta_1^{-\frac12|i-j|}$ we obtain

$$\mathbb{P}_{\mathcal{G}}(\hat{\Delta}_{i,x}\Delta_{j,y}) = \mathcal{O}\big(\theta^{\frac12|i-j|}\big) + C\theta^{\frac14 n^{0.01}},$$

which implies $\mathbb{P}_{\mathcal{G}}(\mathbf{Z}_x\mathbf{Z}_y) = \mathcal{O}(N)$ as claimed. □

Lastly we sketch the proofs of Propositions 2.1–2.3. The proofs of 2.1 and 2.3 proceed along the lines of the proof of Theorem 8. Namely, first we cut off the abnormally high values of $\mathbf{\Delta}_\varepsilon$, if necessary (i.e. if $t < \varepsilon\ln^{100}\varepsilon$), and then employ the big small block technique. We note that the standard proof of the Central Limit Theorem, in the finite horizon case, does not work here for the following reason. That proof relies on the fact that $\nu_0(\tilde{\mathbf{q}}_n^4)$ is of order $\big[\nu_0(\tilde{\mathbf{q}}_n^2)\big]^2$. In the present case, $\nu_0(\tilde{\mathbf{q}}_n^2) = \mathcal{O}(n|\ln\varepsilon|)$, but the estimate of the fourth moment is more complicated. As we know (see the proof of Lemma 11.3), it is based on three cases: Case 1 makes a contribution of $\sim n\varepsilon^{-1}$, Case 2 makes a contribution of $\sim n^2\ln^2\varepsilon$, and Case 3 is insignificant. We see that for large $n$, Case 2 is dominant and leads to the desired relation $\nu_0(\tilde{\mathbf{q}}_n^4) \sim \big[\nu_0(\tilde{\mathbf{q}}_n^2)\big]^2$. But for small $n$, Case 1 dominates (just like it does in the proof of Lemma 11.3), and this causes an anomalous diffusion.

The proof of Proposition 2.2 goes as follows. The first formula is derived similarly to Theorem 6(d), the second formula – similarly to Proposition 3.1 and the third formula – similarly to Theorem 2(d).

## References


[1] Billingsley P. *Convergence of probability measures,* John Wiley & Sons, Inc., New York-London-Sydney 1968 xii+253 pp.

[2] Bleher P. *Statistical properties of two-dimensional periodic Lorentz gas with infinite horizon*, J. Statist. Phys. **66** (1992), 315–373.

[3] Bunimovich L. A. and Sinai Ya. G. *Statistical properties of Lorentz gas with periodic configuration of scatterers,* Comm. Math. Phys. **78** (1980/81), 479–497.

[4] Bunimovich L. A., Sinai Ya. G., and Chernov N. I. *Statistical properties of two-dimensional hyperbolic billiards,* Russ. Math. Surv. **46** (1991), 47–106.

[5] Chernov N. *Decay of correlations and dispersing billiards*, J. Stat. Phys. **94** (1999), 513–556.

[6] Chernov N. *Sinai billiards under small external forces,* Ann. Henri Poincare **2** (2001), 197–236.

[7] Chernov N. *Sinai billiards under small external forces II*, Ann. Henri Poincare **9** (2008), 91–107.

[8] Chernov N. and Dolgopyat D. *Brownian Brownian Motion-1,* Memoirs AMS **198,** no 927, 2009, (193 pp).

[9] Chernov N. and Dolgopyat D. *Galton Board: limit theorems and recurrence,* to appear in Journal of AMS.

[10] Chernov N. and Dolgopyat D. *Diffusive motion and recurrence on an idealized Galton Board,* Phys. Rev. Lett. **99** (2007), paper 030601.

[11] Chernov N. I., Eyink G. L., Lebowitz J. L. and Sinai Ya. G., *Steady-state electrical conduction in the periodic Lorentz gas*, Comm. Math. Phys. **154** (1993), 569–601.

[12] Chernov N. I., Eyink G. L., Lebowitz J. L. and Sinai Ya. G., *Derivation of Ohm's law in a deterministic mechanical model*, Phys. Rev. Lett. **70** (1993), 2209–2212.

[13] Chernov N. and Markarian R., *Chaotic Billiards*, Mathematical Surveys and Monographs, **127**, AMS, Providence, RI, 2006. (316 pp.)

[14] Chernov N. and Zhang H.-K., *Billiards with polynomial mixing rates.* Nonlineartity, **4** (2005), 1527–1553.

[15] Chernov N. and Zhang H.-K., *Improved estimates for correlations in billiards.* Commun. Math. Phys., **277** (2008), 305–321.

[16] Chernov N. and Zhang H.-K., *On statistical properties of hyperbolic systems with singularities*, submitted, available at `www.math.uab.edu/~chernov`

[17] Dolgopyat D. *Limit theorems for partially hyperbolic systems,* Trans. Amer. Math. Soc. **356** (2004) 1637–1689.

[18] Galton F., *Natural Inheritance,* MacMillan, 1989 (facsimile available at www.galton.org).

[19] Gallavotti G. and Ornstein D., *Billiards and Bernoulli schemes*, Comm. Math. Phys. **38** (1974), 83–101.

[20] Lorentz H. A., *The motion of electrons in metallic bodies*, Proc. Amst. Acad. **7** (1905), 438–453.

[21] Marklof J. and Strmbergsson A. *Kinetic transport in the two-dimensional periodic Lorentz gas,* Nonlinearity **21** (2008), 1413–1422.

[22] Marklof J. and Strmbergsson A. *The distribution of free path lengths in the periodic Lorentz gas and related lattice point problems,* to appear in Ann. Math.

[23] Melbourne I. and Török A. *Statistical limit theorems for suspension flows*, Israel J. Math. **144** (2004), 191–209.
[24] Moran B. and Hoover W., *Diffusion in a periodic Lorentz gas*, J. Stat. Phys. **48** (1987), 709–726.
[25] Pesin Ya. B., *Dynamical systems with generalized hyperbolic attractors: hyperbolic, ergodic and topological properties*, Ergod. Th. Dynam. Sys. **12** (1992), 123–151.
[26] Sataev E. A., *Invariant measures for hyperbolic maps with singularities*, Russ. Math. Surv. **47** (1992), 191–251.
[27] Sinai Ya. G., *Dynamical systems with elastic reflections. Ergodic properties of dispersing billiards*, Russ. Math. Surv. **25** (1970), 137–189.
[28] Szasz D. and Varju T. *Limit Laws and Recurrence for the Planar Lorentz Process with Infinite Horizon,* J. Statist. Phys. **129** (2007), 59–80.
[29] Wojtkowski M. P. *$W$-flows on Weyl manifolds and Gaussian thermostats.,* J. Math. Pures Appl. **79** (2000) 953–974.
[30] Young L.-S. *Dimension, entropy and Lyapunov exponents,* Erg.Th., Dyn. Sys. **2** (1982) 109–124.
[31] Young L.-S. *Statistical properties of dynamical systems with some hyperbolicity*, Ann. Math. **147** (1998) 585–650.

N. Chernov Department of Mathematics, University of Alabama at Birmingham, Birmingham, AL 35294

D. Dolgopyat Department of Mathematics, University of Maryland, College Park, MD 20742